Serb. Astron. J. № 183 (2011), 1 - 35 **UDC 520.36–14**
DOI: 10.2298/SAJ1183001J Invited review

ASTRONOMICAL OPTICAL INTERFEROMETRY. II. ASTROPHYSICAL RESULTS

S. Jankov

Astronomical Observatory, Volgina 7, 11060 Belgrade 38, Serbia
E–mail: *sjankov@aob.rs*

(Received: November 24, 2011; Accepted: November 24, 2011)

SUMMARY: Optical interferometry is entering a new age with several ground-based long-baseline observatories now making observations of unprecedented spatial resolution. Based on a great leap forward in the quality and quantity of interferometric data, the astrophysical applications are not limited anymore to classical subjects, such as determination of fundamental properties of stars; namely, their effective temperatures, radii, luminosities and masses, but the present rapid development in this field allowed to move to a situation where optical interferometry is a general tool in studies of many astrophysical phenomena. Particularly, the advent of long-baseline interferometers making use of very large pupils has opened the way to faint objects science and first results on extragalactic objects have made it a reality. The first decade of XXI century is also remarkable for aperture synthesis in the visual and near-infrared wavelength regimes, which provided image reconstructions from stellar surfaces to Active Galactic Nuclei. Here I review the numerous astrophysical results obtained up to date, except for binary and multiple stars milliarcsecond astrometry, which should be a subject of an independent detailed review, taking into account its importance and expected results at micro-arcsecond precision level. To the results obtained with currently available interferometers, I associate the adopted instrumental settings in order to provide a guide for potential users concerning the appropriate instruments which can be used to obtain the desired astrophysical information.

Key words. instrumentation: interferometers – methods: observational – techniques: high angular resolution

1. INTRODUCTION

The new generation of ground-based instruments for high angular resolution from visual and infrared interferometry provided a qualitatively new information for improving our understanding of various astrophysical objects through the comparison of observational results with the predictions of theoretical models. Althoug the optical interferometry has still some limitations in application to various problems (mainly due to the lack of sufficient signal-to-noise ratio for faint objects), it's range of application shows a significant growth, particularly in the past decade.

In Section 2 of the present paper I review several results that represent important contribution to the study of the Sun and Solar system, while the results concerning the determination of stellar fundamental parameters are presented in Section 3, and related asteroseismological results concerning Non Radially Pulsating stars are described in Section 4. The past decade has seen some astonishing results on stellar rotation, which I present in Section 5. The

related Section 6 concerns Be stars and their circumstellar environements while Section 7 describes achievements in the study of Red giants and Supergiants, considering the case of Betelgeuse as the most representative one. Section 8 deals with the Asymptotic Giant Branch stars, particularly Cepheids and Mira type stars. Some remarkable results obtained in the study of Planetary nebulae and their central stars are presented in Section 9, while Section 10 describes the results concerning Luminous Blue Variables and focusing to η Carinae, probably the most studied star after our Sun. The phenomenon of Novae has been only recently studied by means of optical interferometry and this new results are presented in Section 11. Section 12 is dedicated to Young Stellar Objects, namely Herbig Ae/Be stars, T Tauri stars, FU Orionis stars and Massive Young Stellar Objects, all of them being very important for our understanding of how accretion discs evolve into protoplanetary discs and finally to debris discs and planets. The results concerning debris discs and planet formation are presented in Section 13, while Section 14 treats contributions of optical interferometry to the very poupular search for exoplanets. Section 15 describes the results obtained in the study of Central regions of our Galaxy and Section 16 presents the compilation of contributions dedicated to Active Galactic Nuclei. Since the image reconstruction became one of the most valuable tools which generally contributes to all astrophysical fields treated here, I review some of outstanding results in Section 17. Finally, Section 18 presents the conclusion on this work based on all results obtained up to date.

2. SUN AND SOLAR SYSTEM

The Sun and Solar system have not been the prime candidates for application of astronomical optical interferometry due to to the fact that the spatial resolution is provided by the proximity of this scientific targets. In the past, the single aperture interferometry has been contributing to study of Solar system and Sun; for example, the solar features with sizes of the order of 100 km or smaller were found by means of speckle imaging (Harvey 1972, Harvey and Breckinridge 1973). From observations of photospheric granulation from the disc center to the limb, Wilken et al. (1997) found a decrease of the relative contrast of the center-to-limb granular intensity. A time series of high spatial resolution images revealed the highly dynamical evolution of the sunspot fine structure, namely, umbral dots, penumbral filaments, facular points (Denker 1998). Small-scale brightening in the vicinity of sunspots, was also observed in the wings of strong chromospheric absorption lines. These structures which are concomitant with strong magnetic fields show brightness variations close to the diffraction-limit ($\sim$0.16 arcsec at $\lambda = 550$nm), of the Vacuum Tower Telescope, Observatorio del Teide (Tenerife). With the speckle method, Seldin et al. (1996) found the photosphere to be highly dynamic at scales below 0.3 arcsec. Speckle imaging has been successful in resolving the Pluto-Charon system (Bonneau and Foy 1980), as well as in determining shapes of asteroids (Drummond et al. 1988).

However, the investigation of Sun and Solar system by the means of optical interferometry has stalled, mainly due to the fact that satellite observatories and Solar system probes (which are not limited by atmospheric turbulence) provided a very high spatial resolution. But, the application of interferometry is not excluded as shown by Delbo et al. (2009) who obtained the first successful interferometric measurements of asteroid sizes and shapes by means of the Very Large Telescope Interferometer (VLTI) at European Southern Observatory (ESO), and it's MID-infrared Interferometric instrument (MIDI). They observed, as a typical bench mark, the asteroid (951) Gaspra, visited in the past by the Galileo space probe, and they derived a shape in good agreement with the results coming from the in situ measurements by the Galileo mission (see Fig. 1). They have also observed the asteroid (234) Barbara, known to exhibit unusual polarimetric properties, and they found evidence of a potential binary nature. In particular, their data were best fitted by a system of two bodies of 37 and 21 km in diameter, separated by a center-to-center distance of $\sim$ 24 km (projected along the direction of the baseline at the epoch of their observations).

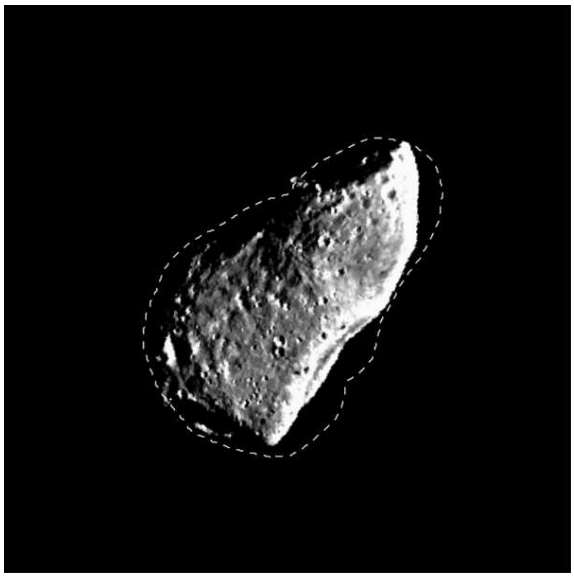

Fig. 1. *Interferometricaly deduced shape and image of (951) Gaspra taken by the Galileo mission. Comparison of an image of (951) Gaspra taken by the Galileo mission on 29/10/1991 at 22:26 UT from a distance of 5300 km and the shape model of Delbo et al. 2009 (dashed line) observed under the same circumstances.*

3. STELLAR FUNDAMENTAL PARAMETERS

Interferometry has long been a valuable tool in the study of stellar physics, primarily in obtaining a broad sample of measurements of fundamental stellar parameters: radius, temperature, luminosity, mass, and chemical composition. However, they are still not well known for a broad range of stellar types. Some properties can be measured by traditional astronomical means. For example, the chemical composition at the surface can be determined by studying spectral lines. A star's temperature can be determined from its luminosity and physical size. To determine the size and the mass, astronomers require extremely high-resolution data that are not easily obtained except by interferometry.

A compilation of direct measurements by high angular resolution methods, as well as indirect estimates of stellar diameters can be found in the Catalog of High Angular Resolution Measurements (CHARM, Richichi and Percheron 2002) which includes most of the measurements obtained by the techniques of lunar occultations and long-baseline interferometry at visual and infrared wavelengths, and which have appeared in the literature or were otherwise made public until mid-2001.

Star's mass is a crucial parameter in stellar astrophysics, however this valuable information cannot be easily obtained directly for a single star. Interferometers bring a new level of resolution to bear on spectroscopic binaries, enabling the full extraction of physical parameters for the component stars with high accuracy. In the case of double-lined systems, a geometrically determined orbital parallax becomes available as presented in the CHARA (Center for High Angular Resolution Astronomy) Catalog of Orbital Elements of Spectroscopic Binary Stars (Taylor et al. 2003).

Using the Mark III Stellar Interferometer on Mount Wilson, Mozurkewich et al. (2003) obtained observations of 85 stars at wavelengths between 451 and 800 nm. Angular diameters were determined by fitting a uniform-disc model to the visibility amplitude versus projected baseline length. Half the angular diameters determined at 800 nm have formal errors smaller than 1 %. Further, the VLTI interferometer and its VINCI and AMBER near-infrared recombiners were used, together with literature measurements, to examine the luminosity-radius and mass-radius relations for K and M dwarfs, Demory et al. (2009) obtained the precision of interferometric radii which competes with what can be obtained for double-lined eclipsing binaries.

Following this work, an updated Catalog of High Angular Resolution Measurements (CHARM2), which includes results available until July 2004, has been presented by Richichi et al. (2005) and complemented by the catalog of the angular sizes of dwarf stars and subgiants (Kervella et al. 2008) who compiled the existing long-baseline interferometric observations of nearby dwarf, and subgiant stars and the corresponding broadband photometry in the Johnson and Cousins bands. For the Hyades giants, γ , δ^1, ϵ, and θ^1Tau, from interferometric measurements with the CHARA Array, Boyajian et al. (2009) deduced the limb-darkened angular diameters with errors less than 2 %. In combination with additional observable quantities, they determined the effective temperatures, linear radii, and absolute luminosities for each of these stars, providing a new calibration of effective temperatures with errors well under 100 K.

At this precision level, the study of stellar atmospheres became possible as shown by Wittkowski et al. (2004a) who presented K-band interferometric measurements of the limb-darkened intensity profile of the M4 giant star ψ Phoenicis obtained with the VLTI/ VINCI instrument. High-precision squared visibility amplitudes in the second lobe of the visibility function were obtained employing two 8.2 m Unit Telescopes. In addition, they sampled the visibility function at small spatial frequencies using the 40cm test siderostats (see Fig. 2). Their measurement constrained the diameter of the star and its center-to-limb intensity variation, as well as (together with the Hipparcos parallax and evolutionary models) stellar mass and surface gravity.

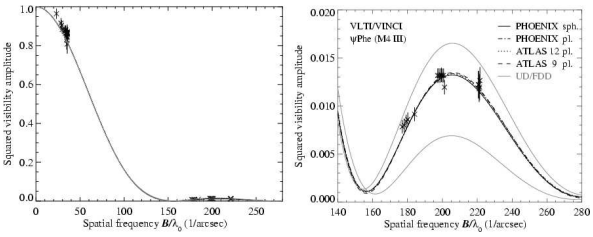

Fig. 2. *ψ Phe diameter and limb darkening determination. The left panel shows the full range of the visibility function while the right panel is an enlargement of the low squared visibility amplitudes in the second lobe. Measured squared visibility amplitudes of ψ Phe are shown (symbols with error bars) together with the (solid black line) spherical radiative transfer model prediction with model parameters $T_{\rm eff}$log g and mass as derived from spectrophotometry and model evolutionary tracks, and best fitting angular diameter value. Shown are also the (dotted and dashed-dotted line) two plane-parallel radiative transfer models, all with corresponding model parameters and best fitted angular diameter. As a reference for the strength of the limb-darkening, the gray lines denote the corresponding uniform disc (upper line) and full darkened disc (lower line) model visibility functions.*

Van Belle et al. (2007) performed the direct angular size measurements of the G0 IV subgiant η Boo from the Palomar Testbed Interferometer (PTI), deducing a limb-darkened angular size of a bolometric flux which provided an effective temperature and luminosity for this object. In conjunction with the mass estimate from the MOST asteroseismology satellite investigation, a surface gravity is established for this star. Using the Infrared Optical Telescope Array (IOTA) and it's IONIC3 recombiner, Lacour

et al. (2008) performed spectro-interferometric observations (R = $\lambda/\Delta\lambda \approx 35$) of Arcturus. Image reconstruction was performed using two software algorithms: Wisard and Mira (e.g. Thiebaut and Giovannelli 2010). No companion was detected from the closure phases with an upper limit on the brightness ratio of $8x10^{-4}$ at 1 AU. The upper limit was also derived for the level of brightness asymmetries present in the photosphere.

The high precision of direct measurements of stellar angular diameter by the VINCI instrument on VLTI stimulated studies which allow the applications in the asteroseismology: Kervella et al. (2003a) compared the first direct angular diameter measurements obtained on α Centauri to recent model diameters constrained by asteroseismic observations. The angular diameters of the two main components of the system (α Cen A and B), were measured with a relative precision of 0.2% and 0.6% respectively while Bigot et al. (2006) improved the angular diameter of α Cen B using limb-darkening predictions from a 3D hydrodynamical radiative transfer model of its atmosphere to fit the interferometric visibility measurements. Pijpers et al. (2003) have studied the radius of the nearby star τ Cet and the limb-darkened disc diameter is determined with an internal precision of 0.5%. Kervella et al. (2003b) reported a direct measurement of the angular diameter of the bright star Sirius A. They obtain a uniform disc angular diameter and (in combination with the Hipparcos parallax) a linear diameter. Using the published properties of Sirius A, they derived internal structure models corresponding to ages between 200 and 250 ± 12 Myr.

The prospects for using the asteroseismology of stars were hampered by the large uncertainty in fundamental stellar parameters. Particularly for rapidly oscillating Ap (roAp) results in the literature for the effective temperature ($T_{\rm eff}$) often span a range of 1000 K. In order to reduce systematic errors and improve the $T_{\rm eff}$ calibration of Ap stars Bruntt et al. (2008) performed the first detailed interferometric study of a rapidly oscillating roAp star, α Cir. They used the Sydney University Stellar Interferometer (SUSI) to measure the angular diameter and accurate Hipparcos parallax to determine the radius constraining the bolometric flux from calibrated spectra which determine an effective temperature, and thus provided the first direct determination of the temperature of an roAp star. Further, Bruntt et al. (2010) obtained long-baseline interferometric observations of β CrB using the CHARA/FLUOR instrument. By combining the flux of the A component with its measured angular diameter, they determined the effective temperature $T_{\rm eff}$(A) = 7980 ± 180 K (2.3 %), with uncertainty in effective temperature similar to that of α Cir (± 170 K).

Observing with the CHARA/VEGA spectro-interferometer, Bigot et al. (2011) measured the angular diameter of the CoRoT satellite target HD49933. A three-dimensional radiative hydrodynamical modeling was used to compute the limb darkening and to derive a reliable diameter. The other fundamental stellar parameters (mass, age, and $T_{\rm eff}$) were found by fitting the large and small p-mode frequency separations using a stellar evolution model.

4. NON RADIALLY PULSATING STARS

The important observational constraints are necessary for detailed studies of the atmospheric structure and pulsation as shown by Kervella et al. (2004a) who reported the angular diameter measurement obtained with the VLTI/VINCI instrument on the nearby star Procyon A (α CMi A, F5IV-V), at a relative precision of ± 0.9 %. They used deduced linear diameter (with the Hipparcos parallax) in combination with the spectroscopic, photometric and asteroseismic data to constrain the model of this star: age, an initial helium mass fraction Y_i, and an initial mass ratio of heavy elements to the hydrogen. They also computed the adiabatic oscillation spectrum of Procyon A giving a mean large frequency separation in agreement with the seismic observations by Martić et al. (2004). The interferometric diameter and the asteroseismic large frequency spacing together suggest a mass closer to 1.4 $M_\odot$ rather than to 1.5 $M_\odot$. From this analysis, they conclude that Procyon is currently ending its life on the main sequence, as its luminosity class indicates. Thévenin et al. (2005) used VLTI/VINCI angular diameter measurements and constrained the evolutionary status of three asteroseismic targets: δ Eri, ξ Hya, η Boo. The main stellar modeling parameters: mass, age and metallicity were adjusted to fit observational data (effective temperature $T_{\rm eff}$, luminosity L and surface metallicity $[Z/X]_{\rm surface}$). In Fig. 3 representing the zoom

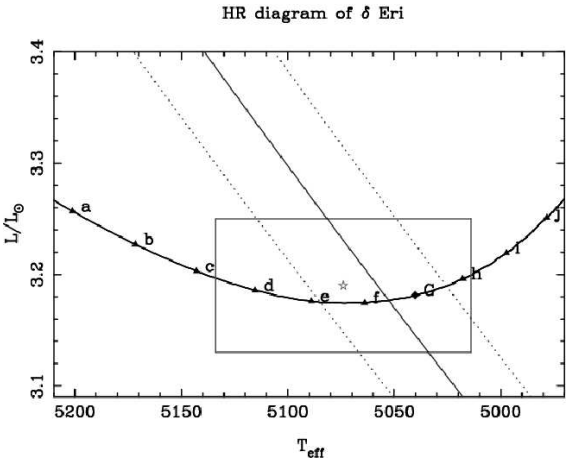

Fig. 3. *δ Eri evolutionary status and asteroseismology. Zoom of the evolutionary tracks in the H-R diagram for δEri from label "a" (6140 Myr) to label "j" (6230 Myr), shown by lower case letters and triangles with time steps of 10 Myr (except label "G" at 6200 Myr labeled by an upper case letter). The rectangular error boxes are derived from the values and accuracies of the adopted stellar parameters while the measured radius and its confidence interval appear as diagonal lines. The best model is close to label "f" at 6194 Myr. The mean large frequency splitting found for the best model is 45.27 μHz.*

of evolutionary tracks on HR diagram for δ Eri, the rectangular error boxes are derived from the values and accuracies of the adopted stellar parameters while the measured radius and its confidence interval (appearing as diagonal lines) allowed the accurate determination of stellar evolutionary status.

Measuring the visual orbit with the Mark III optical interferometer and the Navy Prototype Optical Interferometer (NPOI), combining it with the Hipparcos proper-motion-based parallax and determining the masses and magnitude difference of the components of the Hyades spectroscopic binary θ^2 Tauri, Armstrong et al. (2006) found that both components appear to be less massive and/or brighter than predicted from some recent evolutionary models. The small scale of the λ Vir orbit ($\sim$ 20 mas) was resolved by Zhao et al. (2007) using the IOTA interferometer which, together with spectroscopic data, allowed to determine its elements, as well as the physical properties of the components. The accurately determined properties (0.7% and 1.5% errors, for A and B component respectively) allowed comparisons between observations and current stellar evolution models, and reasonable matches are found. The best-fit stellar model gives λ Vir a subsolar metallicity of Z=0.0097 and an age of 935 Myr. The orbital and physical parameters of the star also allowed to study its tidal evolution timescales and status.

North et al. (2007) used the Sydney University Stellar Interferometer (SUSI) to measure the angular diameter of β Hydri. This star is a nearby G2 subgiant whose mean density was measured with high precision using asteroseismology. They determined the radius and effective temperature of the star and, by combining the radius with the mean density, made a direct estimate of the stellar mass finding a value of $1.07 \pm 0.03 M_{\odot}$(2.8 %). This value agrees with published estimates based on fitting in the Hertzsprung-Russell diagram but has much higher precision, which places valuable constraints on theoretical models of β Hyi and its oscillation frequencies. Mazumdar et al. (2009) studied the GIII red giant star ϵ Oph which has been found to exhibit several modes of oscillation by the MOST satellite. They interpret the observed frequencies of oscillation in terms of theoretical radial p-mode frequencies of stellar models, and evolutionary models of this star, in both the shell H-burning and core He-burning phases of evolution, are constructed. They also obtained an independent estimate of the photospheric radius with highly accurate interferometric observations in the infrared K' band (1.9-2.3 μm) by using the CHARA/FLUOR instrument together with the Hipparcos parallax. The radius obtained from the asteroseismic analysis matched the interferometric value quite closely even though the radius was not constrained during the modeling.

However, with classical interferometric arrays it is possible to resolve spatially only a limited number of nearby bright stars and even more difficult to measure the radii with sufficient precision for asteroseismology. On the other hand, the high resolution spectroscopy allows for (through Doppler Mapping) indirect observational information on atmospheric structures of an unresolved star by modeling the observed flux distribution across the spectral lines. For instance, the differential interferometry (Beckers 1982, Petrov 1988) makes it possible to measure the shift of the stellar photometric barycenter (photocenter) of an unresolved star as a function of wavelength, providing the first order moment of the spatial brightness distribution in addition to the zero order moment spectroscopic information, and allowing better spatial resolution of non-radial stellar pulsations when compared to the classical interferometric and Doppler imaging methods (Jankov et al. 2001, 2002).

Despite of a remarkable progress in understanding stellar interiors, we know surprisingly little about the internal structure of stars spinning near their critical limit. New interferometric imaging of these rapid rotators (see Section 5.) combined with advances in asteroseismology promises to lift this veil and probe the strongly latitude-dependent photospheric characteristics and even reveal the internal angular momentum distribution of these objects. Using the physical properties of α Oph, recently determined from long-baseline interferometry data from the CHARA Array, and the high-precision photometry (based on 30 continuous days of monitoring using the MOST satellite) of this rapidly rotating δ Scuti variable star, Monnier et al. (2010) have identified 57 ± 1 distinct pulsation modes. Remarkably, they have also discovered that the fast rotation modulates the low-frequency modes identified as a rich family of g-modes ($|m|$ up to 7). They found that the spacing of the g-modes is surprisingly linear considering Coriolis forces which are expected to strongly distort the mode spectrum suggesting prograde "equatorial Kelvin" waves (modes $l = m$).

5. RAPIDLY ROTATING STARS

Optical long baseline interferometry is a powerful tool to study detailed stellar shapes. In particular, a rapid rotation induces interferometric signatures requiring a detailed modeling to correctly interpret high angular resolution data. Domiciano de Souza et al. (2002) studied the effects of uniform stellar rotation on interferometric observables using a physically coherent model that includes gravity darkening and geometrical deformation, as well as a radiation transfer code. They investigated the use of multi-baseline and/or multi-wavelength-channel observations, both in the continuum and spectral lines, in order to obtain the unique solutions for relevant model parameters. They showed that this is possible and provided a guide for observers to perform this task. Soon after, Domiciano de Souza et al. (2003) reported the first observations of a rapidly rotating Be star Achernar (α Eridani), using the Earth-rotation synthesis on the VLTI (Fig. 4). Their measurements correspond to an $a/b = 1.56 \pm 0.05$ apparent oblate star (Fig. 5), a and b being the equivalent uniform disc angular radii in the equatorial and polar direction respectively. Considering the presence

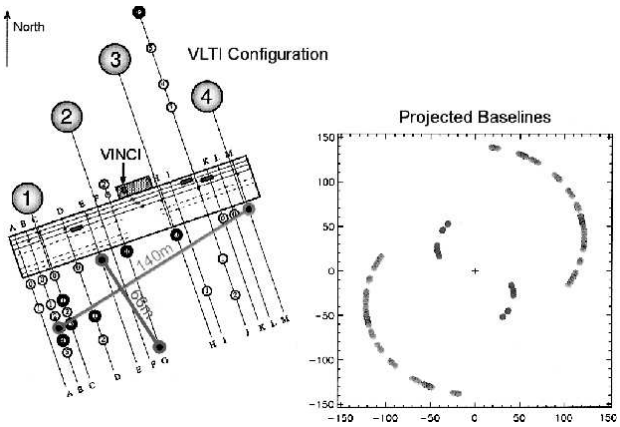

Fig. 4. *Achernar's observations with VLTI/VINCI. VLTI ground baselines for Achernar observations and their corresponding projections onto the sky at different observing times. Left: Aerial view of VLTI ground baselines for the two pairs of 40 cm siderostats used for Achernar observations. Right: Corresponding baseline projections onto the sky as seen from the star.*

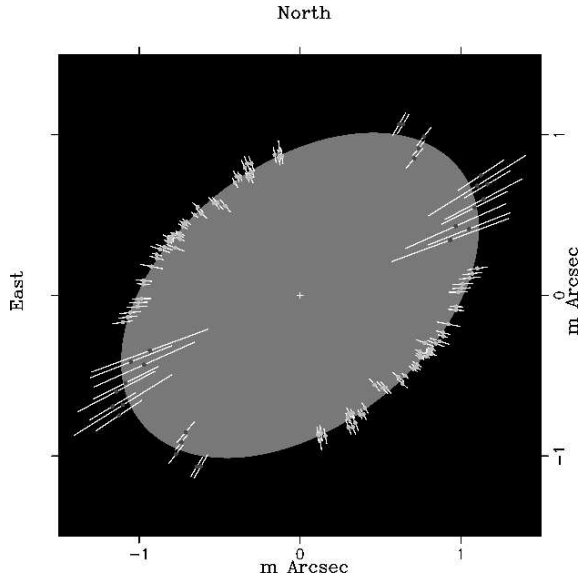

Fig. 5. *Achernar's shape reconstruction. Fit of an ellipse over the observed squared visibilities of Achernar translated to equivalent uniform disc angular diameters. Each value is plotted together with its symmetrical azimuthal value. The fitted ellipse reveals an extremely oblate shape with an equatorial to polar ratio* $a/b = 1.56 \pm 0.05$.

of a circumstellar envelope they argued that their measurement corresponds to a truly distorted star, since α Eridani exhibited a negligible Hα emission during their interferometric observations. In this framework, they conclude that the commonly adopted Roche approximation (uniform rotation and centrally condensed mass) should not apply to this star. This result opened new perspectives to basic astrophysical problems such as the rotationally enhanced mass loss and internal angular momentum distribution. In addition to its intimate relation with magnetism and pulsation, a rapid rotation thus provides a key to the Be phenomenon (see Section 6): one of the outstanding non-resolved problems in stellar physics.

This astonishing result has been confirmed theoretically (Jackson et al. 2004) and observationally: McAlister et al. (2005) reported K-band interferometric observations of the bright, rapidly rotating star Regulus (type B7 V) made with the CHARA interferometer, deducing a high stellar obleteness of 1.32 ± 0.06 (Fig. 6).

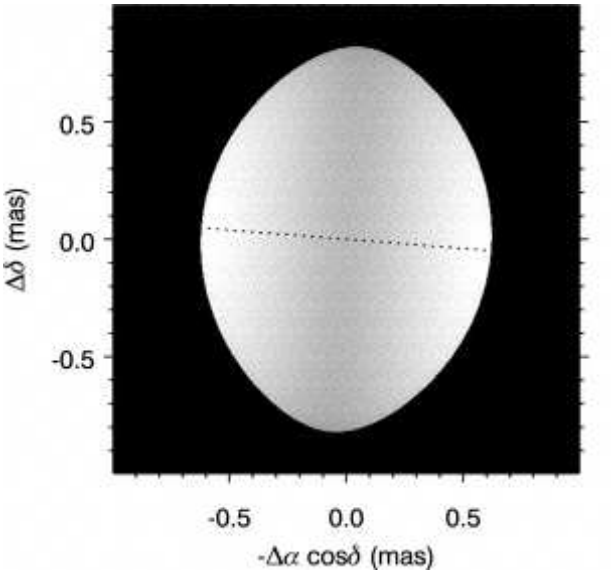

Fig. 6. *K-band image of Regulus. The fitted ellipse revealed an extremely oblate shape with an equatorial to polar ratio* 1.32 ± 0.06.

Infrared interferometric angular size measurements using narrowband channels in the spectrometer at PTI (Palomar Testbed Interferometer, Mt Palomar), indicated a non-circular projected disc brightness distribution for the A7IV-V star Altair (val Belle et al. 2001). Given the known rapid rotation of this star, they modeled the data as arising from an elongated rigid atmosphere. To the first order, an ellipse with an axial ratio of a/b=1.140 $\pm$ 0.029 could be fitted to their interferometric diameter measurements. In addition, Ohishi et al. (2004) reported an asymmetric surface brightness distribution of this rapidly rotating star measured by the NPOI instrument. The outstanding characteristics of these observations were the high resolution with the minimum fringe spacing of 1.7 mas, easily resolving the 3 mas stellar disc, and the measurement of the closure phase, which is a sensitive indicator of the asymmetry of the brightness distribution of the source. They fitted the measured observables to a model with a bright spot on a limb-darkened disc

and found that the observations are well reproduced by a bright spot which has relative intensity of 4.7 %, on the limb-darkened stellar disc. Rapid rotation of Altair indicated that this bright region is a pole, which is brighter than other part of the star owing to gravity darkening. Including new data (squared visibilities in the H and K bands from VLTI/VINCI) as well as previously published data (squared visibilities in the K band from PTI and squared visibilities, triple amplitudes, and closure phases in the visible from NPOI), Domiciano de Souza et al. (2005) showed that the observations can only be explained if Altair has a gravity-darkening compatible with the expected value for hot stars, i.e., the von Zeipel effect ($T_{\rm eff} \sim g^{0.25}$).

Van Belle et al. (2006) presented observations of the A7 IV-V star Alderamin (α Cep) from the CHARA Array. The infrared interferometric angular size measurements indicated a non-circular projected disc brightness distribution for this rapid rotator. The interferometric observations were modeled as arising from an elongated rigid atmosphere with an axial ratio of 1.298 ± 0.051. The inclination of Alderamin to the line of sight indicated by this modeling is ($i = 88.2^{\circ}{}^{+1.8}_{-13.3}$) and the star has a rotational velocity which is ~ 83 % of breakup velocity. A remarkable aspect of this modeling was a determination of the gravity-darkening coefficient which, at a value of $\beta = 0.084^{+0.026}_{-0.049}$, is consistent with a convective photosphere as expected for an A7 IV-V star.

Peterson et al. (2006a) reported the successful fitting of a Roche model with a surface temperature gradient following the von Zeipel gravity darkening law to observations of Altair made with the Navy Prototype Optical Interferometer. They confirm the claim by Ohishi et al. (2004) and Domiciano de Souza et al. (2005) that Altair displays an asymmetric intensity distribution due to rotation. The modeling indicated that Altair is rotating at 0.90 ± 0.02 of its breakup (angular) velocity. Their results are consistent with the apparent oblateness found by van Belle et al. and show that the true oblateness is significantly larger owing to an inclination of the rotational axis of $\sim 64^{\circ}$. Of particular interest, they conclude that instead of being substantially evolved as indicated by its classification A7 IV-V, Altair is only barely off the zero-age main sequence and represents a good example of difficulties rotation can introduce in the interpretation of this part of the HR diagram.

Peterson et al. (2006b) reported a closure phase optical interferometric observations at the NPOI that show that Vega has the asymmetric brightness distribution of the bright, slightly offset polar axis of the star rotating at 93% of its breakup velocity. In addition to explaining the unusual brightness and line shape peculiarities, this result leads to the prediction of an excess of near-infrared emission compared to the visible, in agreement with observations. The large temperature differences predicted across its surface call into question composition determinations, adding uncertainty to Vega's age and opening the possibility that its debris disc could be substantially older than previously thought. Yoon et al. (2008) reported a reanalysis of Vega's composition. A full spectral synthesis based on the Roche model derived earlier from NPOI interferometry is used. They find the line shapes in Vega's spectrum to be more complex than just flat-bottomed, which have been previously reported. They investigate the effects of rotation on the deduced abundances and show that the dominant ionization states are only slightly affected compared to analyses using nonrotating models. They argue that the rapid rotation requires the star to be fully mixed. This composition leads to masses and particularly ages that are quite different compared to what were usually assumed.

Zhao et al. (2009) presented sub-milliarcsecond resolution imaging and modeling of two nearby rapid rotators, α Cephei and α Ophiuchi, obtained with the CHARA array. Incorporating a gravity-darkening model, they determine the inclination, the polar and equatorial radius and temperature, as well as the fractional rotation speed of the two stars with unprecedented precision. The polar and equatorial regions of the two stars have ~ 2000 K temperature gradient causing their apparent temperatures and luminosities to be dependent on their viewing angles. Their modeling (Fig. 7) allowed to determine the true effective temperatures and luminosities of α Cep and α Oph permitting to investigate their true locations on the H-R diagram. These properties in turn give estimates of the masses and ages of the two stars within a few percent of error using stellar evolution models. Also, based on their gravity-darkening modeling, they propose a new method to estimate the masses of single stars in a more direct way through $V_{\rm e} \sin i$ measurements and precise geometrical constraint.

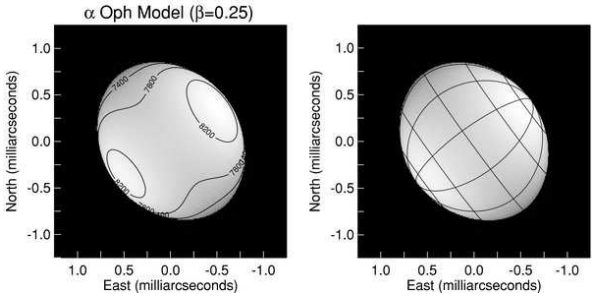

Fig. 7. *Best-fit standard gravity-darkening model of α Oph. The contours in the left panel indicate the local brightness temperatures on the surface of the star. The right panel shows the latitude and longitude of α Oph to help visualize its geometry.*

An alternative approach to study the rapidly rotating stars has been proposed by Jankov et al. (2003a and 2003b) who considered the case of stellar activity, showing the potential of new methods which combine the classical spectroscopy (Tomographic Imaging) and Long Baseline Interferometry, providing informations that cannot be obtained otherwise by each of these techniques taken separately. By

means of numerical simulations, Rousselet-Perraut et al. (2004) investigated the ability of optical interferometry via the fringe phase observable to address stellar activity and magnetism. To derive abundance maps and stellar rotation axes they use the color differential interferometry which couples high angular resolution to high spectral resolution while, to constrain magnetic field topologies, they add a polarimetric mode. They emphasize the crucial need for developing and validating inversion algorithms so that future instruments on optical aperture synthesis arrays can be optimally used.

6. Be STARS

Be stars show evidence of mass loss and circumstellar envelopes (CSE) from UV resonance lines, near-IR excesses, and the presence of episodic hydrogen emission lines. The geometry of these envelopes is still uncertain, although it is often assumed that they are formed by a disc around the stellar equator and a hot polar wind. This envelope emission is more extended, and thus more easily resolvable, than the tiny photosphere itself. The envelope of γ Cas was first resolved by Thom et al. (1986) using the I2T interferometer, and Mourard et al. (1989) using the GI2T interferometer. The high spectral resolution of GI2T later also uncovered asymmetric emission in these Be star envelopes in Hα (Stee et al. 1995), and observed in other lines too (Stee et al. 1998). Vakili et al. (1998) proposed that the emission line region is very one-sided and time-variable.

With a good range of baselines, the Mark III interferometer was able to detect definite asymmetries in γ Cas and ζ Tau (Quirrenbach et al. 1993, 1994) while Tycner et al. (2004) presented optical interferometric observations of ζ Tau obtained using the NPOI. The observations suggested a strong departure from circular symmetry which has been described by an elliptical model. Tycner et al. (2005) presented the long-baseline interferometric observations, obtained with the NPOI, of the Hα-emitting envelopes of the Be stars η Tau and β CMi, demonstrating a clear dependence of the net Hα emission on the linear size of the emitting region. These results are consistent with an optically thick line emission that is directly proportional to the effective area of the emitting disc. Chesneau et al. (2005a) presented the first VLTI/MIDI observations of the Be star α Ara showing a nearly unresolved circumstellar disc in the N band. These measurements put an upper limit on the envelope size corresponding to 14 R_* assuming R_*=4.8 $R_\odot$ and the Hipparcos distance of 74 pc. These observations also placed complementary constraints on the density and geometry of the α Ara circumstellar disc.

Tycner et al. (2006) presented interferometric observations of two well-known Be stars, γ Cas and φ Per, collected and analyzed to determine the spatial characteristics of their circumstellar regions. The observations were obtained using the NPOI equipped with narrowband filters which isolate the Hα emission line from the nearby continuum radiation, resulting in an increased contrast between the interferometric signature due to the Hα-emitting circumstellar region and the central star, thus allowing the interferometric signal in the Hα channel to be calibrated with respect to the continuum channels. The observations used in this study represent the highest spatial resolution measurements of the Hα-emitting regions of Be stars obtained to date. These observations allowed them to demonstrate for the first time that the intensity distribution in the circumstellar region of a Be star cannot be represented by a uniform disc or ring-like structures whereas a Gaussian intensity distribution appeared to be fully consistent with their observations. Kervella and Domiciano de Souza (2006a) presented long-baseline interferometric observations of Achernar with the VLTI/VINCI beam recombiner in the H and K bands by using various telescope configurations and baseline lengths with a wide azimuthal coverage. They clearly detected a CSE elongated along the polar axis of the star as well as rotational flattening of the stellar photosphere. They conclude that this CSE could be linked to free-free emission from the radiative pressure driven wind originating from the hot polar caps of the star.

Gies et al. (2007) presented the first K'-band, long-baseline interferometric observations of the Be stars γ Cas, φ Per, ζ Tau, and κ Dra. The measurements were made with multiple telescope pairs of the CHARA interferometer resolving the circumstellar discs of the targets. The disc resulting densities are in broad agreement with prior studies of the IR excess flux, and the resulting orientations generally agree with those from interferometric Hα and continuum polarimetric observations. They find that the angular size of the K' disc emission is smaller than that determined for the Hα emission, and they argue that the difference is the result of a larger Hα opacity and the relatively larger neutral hydrogen fraction with increasing disc radius. Domiciano de Souza et al. (2007) presented the first high spatial and spectral resolution observations of the circumstellar envelope of a B[e] supergiant (CPD-57°2874), performed with the VLTI. Spectra, visibilities and closure phase were obtained using the beam-recombiner instruments AMBER, near-IR interferometry with three 8.3 m Unit Telescopes (UTs) and MIDI with two UTs. The interferometric observations of the CSE are well fitted by an elliptical Gaussian model with FWHM diameters varying linearly with wavelength. The major-axis position angle of the elongated CSE in the mid-IR agrees well with previous polarimetric data, hinting that the hot-dust emission originates in a disc-like structure and supporting the non-spherical CSE paradigm for B[e] supergiants.

Using the VLTI/AMBER instrument operating in the K-band, Meilland et al. (2007a) studied the geometry and kinematics of the disc around the Be star α Arae as a function of wavelength, especially across the Brγ (λ 2.1657 μm) emission line, which provided a gain by a factor of 5 in spatial resolution compared to previous VLTI/MIDI observations. Consequently, it was possible to combine the high angular resolution provided with the medium (R$\sim$ 1500) spectral resolution of AMBER to study the kinematics of the inner part of the disc and to in-

fer its rotation law. For the first time, they obtained direct evidence that the disc is in the Keplerian rotation, answering the question that has existed since the discovery of the first Be star (γ Cas). They found that the disc around α Arae is compatible with a dense equatorial matter confined to the central region whereas a polar wind is contributing along the rotational axis of the central star (Fig. 8).

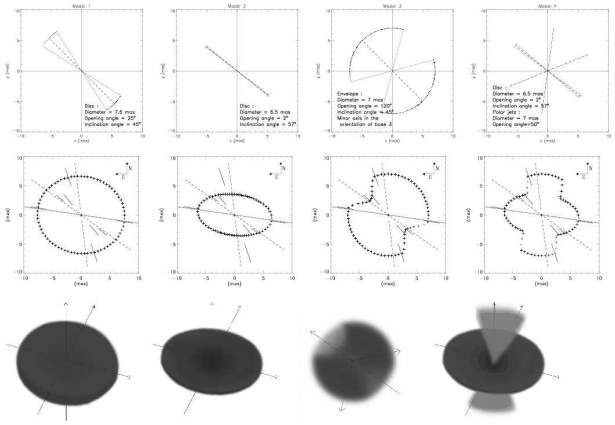

Fig. 8. *Models of α Arae. The four upper panels are a cut of the circumstellar disc in a plane defined by the observer line of sight and the stellar rotational axis (the observer is on the right in each picture); the corresponding projections onto the sky-plane with the interferometric data points from MIDI and AMBER over-plotted are the central pictures, whereas a 3Dview' is plotted into the lower row for each model.*

Meilland et al. (2007b) observed with VLTI/AMBER the circumstellar environment of the Be star κ CMa in the Brγ emission line and its nearby continuum to study the kinematics within the disc and to infer its rotation law. Using differential visibilities and differential phases across the Brγ line they detected an asymmetry in the disc (see Fig. 9). Moreover, they found that κ CMa seems difficult to fit within the classical scenario for Be stars, illustrated by previous α Arae observations, i.e. a fast rotating B star close to its breakup velocity surrounded by a Keplerian circumstellar disc with an enhanced polar wind. They discuss the possibility that κ CMa is a critical rotator with a Keplerian rotating disc and examine whether the detected asymmetry can be interpreted within the "one-armed" viscous disc framework.

Meilland et al. (2008) studied the Be star δ Cen circumstellar disc in the H and K band using low (R=35) and medium (R=1500) spectral resolution observations. They detected an oscillation in the visibility curve plotted as a function of the spatial frequency which is a clear signature of a companion around the star. They also report an envelope flux around the Be primary that contributes up to about 50 % of the total flux, in agreement with Spectral Energy Distribution (SED). The envelope size was estimated but no departure from spherical symmetry was detected.

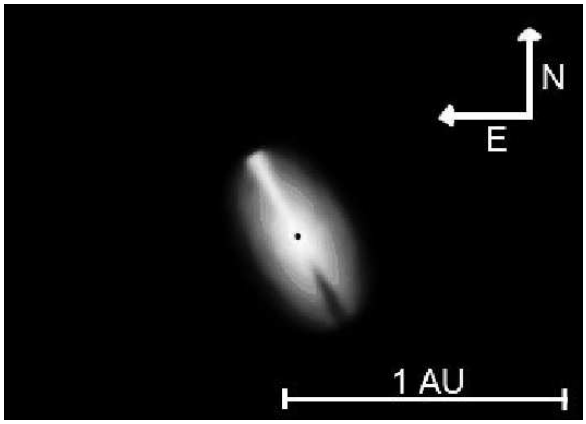

Fig. 9. *κ CMa intensity map in the continuum at 2.15μm. The inclination angle is 60°, the central black dot represents the κ CMa photosphere (0.25mas).*

Using the VLTI/VINCI instrument, Carciofi and Domiciano de Souza (2008) performed a new interferometric study of Achernar, identifying two different disc models that simultaneously fit the spectroscopic, polarimetric, and interferometric observational constraints: a tenuous disc in hydrostatic equilibrium (i.e. with small scale height) and a smaller, scale height enhanced disc. They concluded that these relatively small discs correspond to the transition region between the photosphere and the circumstellar environment and that they are probably perturbed by some photospheric mechanism.

Kervella et al. (2009) searched for the signature of circumstellar emission at distances of a few stellar radii from Achernar, in the thermal IR domain. They obtained interferometric observations on three VLTI baselines in the N band (8-13 μm), using the MIDI instrument. From the measured visibilities, they derive the angular extension and flux contribution of the N band circumstellar emission in the polar direction of Achernar. This flux contribution is in good agreement with the photometric IR excess measured by fitting the spectral energy distribution. They concluded that this polar envelope, already detected at 2.2 μm, is most probably an observational signature of the fast wind ejected by the hot polar caps of the star.

Meilland et al. (2009) obtained calibrated visibility measurements for stars: p Car, ζ Tau, κ CMa, α Col, δ Cen and β CMi, α Ara, using the VLTI/MIDI instrument in the N band. They compared their results with previous K band measurements obtained with the VLTI/AMBER instrument and/or the CHARA interferometer, concluding that the size of the circumstellar envelopes for these classical Be stars does not seem to vary strongly on the observed wavelength between 8 and 12 μm. Millan-Gabet et al. (2010) presented near-infrared H and K-band spectro-interferometric observations of the gaseous disc around the primary Be star in the δ Sco binary system. Using observations at the CHARA/MIRC instrument in the H band they resolved an elongated disc, while using the Keck Inter-

ferometer (KI) the source of the K-band continuum emission was only marginally spatially resolved. On the other hand, the line emission in He I λ 2.0583 μm and Brγ, was clearly detected with ~ 10 % lower visibilities than those of the continuum. When taking into account the continuum/line flux ratio this translates into much larger sizes for the line emission regions. Their KI data also reveal a relatively flat spectral differential phase response, ruling out a significant off-center emission.

Meilland et al. (accepted 2011) carried out observations of the sample composed of eight bright classical Be stars: α Col, κ CMa, ω Car, p Car, δ Cen, μ Cen, α Ara, and o Aqr, with the VLTI/AMBER instrument combining high spectral (R=12000) and high spatial ($\theta_{\rm min}$=4 mas) resolutions. They determined the disc extension in the line and the nearby continuum for most targets, constraining the disc kinematics and showing that it is dominated by rotation with a rotation law close to the Keplerian one. The survey also suggests that these stars are rotating below their critical velocities (V_c) with a mean rotational rate of 0.82±0.08 V_c, leading to the conclusion that their Be stars sample suggests that the rotation alone cannot explain the origin of the Be phenomenon and that other mechanisms are playing a non-negligible role in the ejection of matter.

7. RED GIANTS AND SUPERGIANTS: Betelgeuse

Historically, red giants and supergiants were one of the favorite targets for stellar interferometry, and there are many of them for which the fundamental parameters are precisely derived. However, the most famous case in the quest for surface inhomogenities in giants stars is the M2 supergiant Betelgeuse (α Ori). The interferometry research to study the inhomogenities of stellar surfaces began by using (visible-light) aperture masking on the William Herschel telescope in the Canary Islands (Baldwin et al. 1986, Haniff et al. 1987). Interferometric non-redundant masking imaging was performed and early results showed bright features (strong departure from circular symmetry) on the surface of the Betelgeuse (Buscher et al. 1990), confirming some previous reports (e.g. Roddier and Roddier 1983). No long baseline (separate-element) interferometer would be able to investigate the nature of these features for years, and the Cambridge masking group has spent more than a decade thoroughly investigating "hotspots" on red supergiants and giants. Over the two last decades, it was shown that asymmetries are common (although not omnipresent) around red supergiants and giants at visible wavelengths (Wilson et al. 1992, Tuthill et al. 1997, 1999), that these hotspots vary on a timescale of months (Wilson et al. 1997), and that the asymmetries become less-pronounced (even disappearing) into the IR (Young et al 2000). However, the first image of a stellar photosphere using optical aperture synthesis with the Cambridge Optical Aperture Synthesis Telescope (COAST) interferometer showed a featureless (uniform and circularly symmetric disc) Betelgeuse (Burns et al. 1997).

Ohnaka et al. (2009) presented spatially resolved, high-spectral resolution K-band observations of the Betelgeuse using VLTI/AMBER in order to probe inhomogeneous structures in the dynamical atmosphere of the star. Betelgeuse was observed in the wavelength range between 2.28 and 2.31 μm with spectral resolutions of 4800-12000 allowing to study inhomogeneities seen in the individual CO first overtone lines. The data could roughly be explained by a simple model in which a patch of CO gas is moving outward or inward with velocities of 10-15 km s^{-1}, while the CO gas in the remaining region in the atmosphere is moving in the opposite direction at the same velocities. Also, the data are consistent with the presence of warm molecular layers extending to 1.4-1.5 R_*. Haubois et al. (2009) reported on H-band interferometric observations of Betelgeuse made by the three-telescope interferometer IOTA. They imaged the star and its asymmetries to deduce the spatial variation of the photosphere, including its diameter, limb darkening, effective temperature, surrounding brightness, and star spots. Resolved images of Betelgeuse in the H band are asymmetric at the level of a few percent while the amount of measured limb-darkening is in good agreement with model predictions. The two spots imaged at the surface of the star are potential signatures of convective cells (Fig. 10).

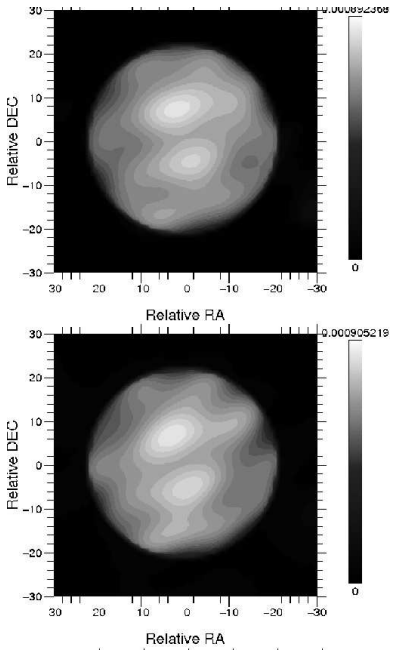

Fig. 10. *Image reconstruction of Betelgeuse. Upper panel: contour image reconstruction of Betelgeuse from MIRA. Lower panel: contour image reconstruction from WISARD of Betelgeuse in a 60 mas field. Both images were reconstructed with the same apriori object and the same type of regularization.*

Ravi et al. (2011) presented an interferometric study of the continuum surface of Betelgeuse at 11μm wavelength, using data obtained with the Berkeley Infrared Spatial Interferometer (ISI) each year between 2006 and 2010. These data allowed an investigation of an optically thick layer within 1.4 R_*, which has an optical depth of $\sim$ 1 at 11 μm, and varies in temperature between 1900 K and 2800 K and in outer radius between 1.16 and 1.36 stellar radii. The layer has a non-uniform intensity distribution that changes between observing epochs. These results indicate that large-scale surface convective activity strongly influences the dynamics of the inner atmosphere of Betelgeuse and mass-loss processes.

8. ASYMPTOTIC GIANT BRANCH STARS

The apparent interferometric sizes of variable red giants vary dramatically up to a factor of 3 with wavelength and pulsation phase (Tuthill et al. 1995, Weiner et al. 2000, Mennesson et al. 2002, Perrin et al. 2004a, Weiner 2004). These large variations challenge the hydrodynamical and line opacity models of these stars indicating that their extended atmospheres are extremely complex. This recently stimulated a large sample of stars to be observed using benefits of high spatial resolution provided by new generation of interferometers. Infrared interferometry of Asymptotic Giant Branch (AGB) stars has recently been reinterpreted as revealing the presence of deep molecular layers. Empirical models for a photosphere surrounded by a simple molecular layer or envelope have led to a consistent interpretation of previously inconsistent data. The stellar photospheres are found to be smaller than previously understood and the molecular layer is much higher and denser than predicted by the hydrostatic equilibrium.

The size of the continuum photospheres of α Ori, α Her, R Leo, and χ Cyg have been measured at 11 μm by Weiner et al. (2003), using heterodyne interferometry (obtained from ISI) to accuracies as high as 1%. The resulting apparent diameters for α Ori and α Her are $\sim$ 30 % larger than measured near-infrared sizes, whereas the Mira variables R Leo and χ Cyg, have 11 μm apparent diameters, roughly twice their reported near-infrared sizes. Mennesson et al. (2005) reported interferometric observations of the semiregular variable star RS CrB, a red giant with strong silicate emission features. The data were among the first long baseline mid-infrared stellar fringes obtained between the Keck telescopes, using parts of the new nulling beam recombiner. The light was dispersed by a low-resolution spectrometer allowing simultaneous measurement of the source visibility and intensity spectra from 8 to 12 μm, and the observations provided a non-ambiguous determination of the dust shell spatial scale and relative flux contribution. Ragland et al. (2006) have measured non-zero closure phases for the sample of 56 nearby AGB stars using the three-telescope IOTA interferometer at near-infrared wavelengths (H band) and with angular resolutions in the range 5-10 mas. Reporting the measured stellar angular sizes, they hypothesize that most Mira stars would show detectable asymmetry if observed with adequate angular resolution since the detected non-zero closure phases can only be generated by asymmetric brightness distributions of the target stars or their surroundings. Deroo et al. (2006) presented the first mid-IR long baseline VLTI/MIDI interferometric observations of the circumstellar matter around binary post-AGB stars, SX Cen and HD 52961, confirming the disc interpretation of the spectral energy distribution of both stars.

8.1. Cepheids

Although phenomenologically related to measurements of pulsating AGB stars, observations of Cepheids are quite distinct in their scientific goals. As has been discussed (e.g. Davis 1976), optical interferometry should play an important role in independent calibration of the Cepheid distance scale, a crucial element of the cosmic distance ladder. By measuring the changing diameter of a nearby Cepheid and the radial velocity curve through a pulsation cycle, the distance can be directly inferred via the Baade-Wesselink method, and unbiased angular diameter measurements are required for accurate distances to Cepheids.

The initial results have appeared from GI2T (Mourard et al. 1997), NPOI (Armstrong et al. 2001), IOTA (Kervella et al. 2001), and PTI (the first direct detection of Cepheid pulsation; Lane et al. 2000). The field is rapidly developing, both observationally and theoretically. Lane et al. (2002) presented observations of the Galactic Cepheids η Aql and ζ Gem, and their observations were able to resolve the diameter changes associated with pulsation. This allows the distance to the Cepheids to be determined independently of photometric observations, providing calibration of surface brightness relations for use in extragalactic distance determination. They also provided a measurement of the mean diameter of these Cepheids which is crucial for constructing reliable structural models of this stellar class. Nordgren et al. (2002) used direct diameter observations of Cepheid variables to calibrate the Barnes-Evans Cepheid surface brightness relation. Fifty-nine separate Cepheid diameter measurements from four different optical interferometers were used to calculate surface brightnesses as a function of magnitude and color. The linear relation to Cepheid surface brightness versus color was in excellent agreement with functions found using interferometric observations of nonvariable giant and supergiant stars. Using these relations, they deduced distance of δ Cephei, and compared it to an independent distance which is known from trigonometric parallax.

Kervella et al. (2004b) reported the angular diameter measurements of seven classical Cepheids, X Sgr, η Aql, W Sgr, ζ Gem, β Dor, Y Oph and l Car, obtained with the VLTI/VINCI instrument. They also used reprocessed archive data obtained with the IOTA/FLUOR instrument on ζ Gem, in order to improve the phase coverage of their observations. They obtained average limb darkened angu-

lar diameters for four of these stars, η Aql, W Sgr, β Dor, and l Car, and they detected the pulsational variation of their angular diameters. This allowed to compute directly their distances, using a modified version of the Baade-Wesselink method. Kervella et al. (2004c) derived new calibrations of the Cepheid period-radius (P-R) and period-luminosity (P-L) relations using the interferometric angular diameter measurements of seven classical Cepheids reported in Kervella et al. (2004b), and complemented by previously existing measurements. Taking advantage of the significantly larger color range covered by these observations, they derived high precision calibrations of the surface brightness-color relations using exclusively Cepheid observations, making it possible to improve the distance to Cepheids through a Baade-Wesselink type technique. However, using this method, the distance is known to a multiplicative factor called the projection factor. This factor has been measured directly, for the first time using interferometry at the CHARA Array by Mérand et al. (2005) who deduced a geometrical measurement of the projection factor of δ Cep.

VLTI observations of the brightest and angularly largest classical Cepheid, l Carinae have resolved with high precision the variation of its angular diameter with phase. Kervella et al. (2004d) compared the measured angular diameter curve to the one that they derive by an application of the Baade-Wesselink-type infrared surface brightness technique and found an almost perfect agreement between the two curves. The mean angular diameters of l Car from the two techniques agree very well within their total error bars (1.5 %) as do the derived distances (4 %) indicating that the calibration of the surface brightness relations used in the distance determination of far-away Cepheids is not affected by large biases. Kervella et al. (2006b) presented the results of long-baseline interferometric observations of l Carinae in the infrared N (8-13 μm) and K (2.0-2.4 μm) bands, using the MIDI and VINCI instruments of the VLT Interferometer. In the N band they resolved a large circumstellar envelope. The signature of this envelope was also detected in the K band data as a deviation from a single limb darkened disc visibility function. Considering a possibility that this CSE is linked to the relatively large mass loss rate of l Car, they discuss an analogy with the molecular envelopes of Red supergiants, and Miras. Mérand et al. (2006) presented the results of long-baseline interferometric observations of the classical Cepheids Polaris (α UMi) and δ Cep in the near infrared K' band, using the CHARA/FLOUR Array. Following their previous detection of a circumstellar envelope around l Car (Kervella et al. 2006b), they report similar detections around Polaris and δ Cep.

Mérand et al. (2007) observed a Cepheid Y Oph for which the pulsation has been well resolved using the long-baseline near-infrared interferometry with CHARA/FLOUR. They found that the observations suggest the star surrounded by a circumstellar envelope with characteristics similar to that found previously around other Cepheids, pointing toward the conclusion that most Cepheids are surrounded by faint circumstellar envelopes. Observations of the southern Cepheid l Car to yield the mean angular diameter and angular pulsation amplitude, have been made with the SUSI array at a wavelength of 696 nm by Davis et al. (2009). The interferometric results have been combined with radial displacements of the stellar atmosphere derived from selected radial velocity data to determine the distance and mean diameter of l Car, showing excellent agreement with previously published values. However, no evidence was found for a circumstellar envelope at 696 nm.

8.2. Miras

Mira variables are low- to intermediate-mass asymptotic giant branch (AGB) stars that pulsate with a period of about one year. They have a cool ($T_{\rm eff} \leq$ 3000 K) and extended ($R > 100 R_*$) photosphere. The circumstellar environment of Mira variable stars is characterized by cool temperatures and relatively high densities leading to a richer chemistry than that found in hotter stars and to formation of solid-state dust grains.

The long-term monitoring of Mira variables at the PTI performed by Thompson et al. (2002a) provided high-resolution narrowband angular sizes of the oxygen-rich Mira S Lac and the carbon-rich Mira RZ Peg in the near-infrared. Their data set spanned three pulsation cycles for S Lac and two pulsation cycles for RZ Peg and represents the first study to correlate multi-epoch narrowband interferometric data of Mira variables. As a part of a long-term observational program using the IOTA Array, van Belle et al. (2002) presented angular size measurements of 22 oxygen-rich Mira variable stars in order to characterize the observable behavior of these stars. A simple examination of the resultant sizes of these stars in the context of pulsation mode was consistent with at least some of these objects pulsating in the fundamental mode.

Thompson et al. (2002b) reported high-resolution ($<$ 0.05 mas) angular size measurements of the Mira variable star R Tri using the PTI in the K band (2.0-2.4 μm), and modeling with simple geometries. For the axially symmetric models, the position angles are roughly perpendicular to visual polarization position angles, which supports an axially symmetric source of light scattering. For the elliptical geometry, the axial ratio of 1.33 has been determined, similar to that previously determined for other Mira and semiregular variable stars.

Mennesson et al. (2002) observed nine bright O-rich Mira stars and five semiregular variable cool M giants with the IOTA interferometer in both K' ($\sim$ 2.15 μm) and L' ($\sim$ 3.8 μm) broadband filters. To explain large apparent diameter increases between the K' and L' bands they propose a simple two-component model consisting of a warm (1500-2000 K), extended (up to $\sim$ 3 stellar radii), optically thin ($\tau \sim 0.5$) layer located above the classical photosphere which could explain the observed variation of Mira uniform disc diameters. This interpretation was consistent with the extended molecular gas layers (H_2O , CO, etc.) inferred around some of these objects from previous IOTA K'-band interferometric

observations. The two-component model had immediate implications: the Mira photosphere diameters are smaller than previously recognized which implies higher effective temperatures, favoring fundamental mode pulsation. Using the same instrument, Hofmann et al. (2002) presented K'-band observations of five Mira stars: M-type Miras: X Oph, R Aql, RU Her, R Ser, and the C-type Mira V CrB. The derived angular Rosseland radii and the bolometric fluxes allowed the determination of effective temperatures which, together with deduced linear radii, confirmed fundamental mode pulsation interpretation.

Perrin et al. (2004b) have observed Mira stars on the IOTA interferometer in narrow bands around 2.2 μm wavelength, finding systematically larger diameters in bands contaminated by water vapor and CO. Their visibility measurements could be interpreted by a model comprising a photosphere surrounded by a thin spherical molecular layer while the deduced photospheric diameters were found smaller than in previous studies by several tens of percent, indicating that all Mira stars are fundamental mode pulsators; the previous studies leading to the conclusion of the first-overtone mode were biased by too large diameter estimates.

Woodruff et al. (2004) presented K-band observations of the Mira star prototype *o* Cet obtained by the VLTI/VINCI instrument and two siderostats. Their comparison of deduced Rosseland radii, effective temperatures, and the shape of the observed visibility functions with model predictions confirmed that o Cet is a fundamental mode pulsator. Ohnaka et al. (2005) presented the results of the first mid-infrared interferometric observations of the Mira variable RR Sco with the VLTI/MIDI, together with K-band observations using VLTI/VINCI. Their model calculations show that optically thick emission from a warm molecular envelope consisting of H_2O and SiO can cause the apparent mid-infrared diameter to be much larger than the continuum diameter. The observed increase of the uniform-disc diameter longward of 10 μm could be explained by an optically thin dust shell consisting of silicate and corundum grains. Millan-Gabet et al. (2005) presented the first spatially resolved observations of a sample of 23 Mira stars simultaneously measured in the near-infrared J, H, and K' bands, using the IOTA interferometer. For each star they present visibility amplitude measurements as a function of wavelength, revealing the general relation: J diameter < H diameter < K' diameter.

Ireland et al. (2005) performed optical interferometric polarimetry measurements of the Mira-like variables R Car and RR Sco, using the SUSI array. By making visibility measurements in two perpendicular polarizations, the relatively low-surface brightness light scattered by atmospheric dust could be spatially separated from the bright Mira photospheric flux. This was the first reported successful use of long-baseline optical interferometric polarimetry. Observations were able to place constraints on the distribution of circumstellar material; the inner radius of dust formation for both stars was found to be less than 3 stellar radii: much closer than the expected innermost stable location for commonly assumed astrophysical "dirty silicate" dust (silicate dust with a significant iron content) in these systems. Fedele et al. (2005) presented near-infrared K-band interferometric measurements of the Mira star R Leonis obtained with the VLTI/VINCI. These measurements indicate a center-to-limb intensity variation that is clearly different from a uniform disc intensity profile. Also, they showed that these measured visibility values are consistent with predictions from recent self-excited dynamic Mira model atmospheres that include molecular shells close to continuum-forming layers. Perrin et al. (2005) reported IOTA/FLUOR interferometry with narrow spectral bands, isolating the near-continuum and strong molecular features, obtained for the supergiant μ Cep. Their model shows that a stellar photosphere of angular diameter 14.11 $\pm$ 0.60 mas is surrounded by a molecular layer of diameter 18.56 $\pm$ 0.26 mas

Boboltz et al. (2005) presented the first coordinated Very Long Baseline Array (VLBA)/Very Large Telescope Interferometer (VLTI) measurements of the stellar diameter and circumstellar atmosphere of a Mira variable star. Observations of the SiO maser emission toward the Mira variable S Ori were conducted using the VLBA, while near-infrared K-band measurements of the stellar diameter were performed using VLTI/VINCI and closely spaced in time to the VLBA observations. Their measurements show that the masers lie relatively close to the stellar photosphere at a distance of $\sim$2 photospheric radii, consistent with model estimates. Weiner et al. (2006) performed mid-infrared observations of IK Tau at 11.15 μm with the three-telescope ISI, and also using individual segments of the Keck telescope for multiple-aperture interferometry at 10.7 μm. Both experiments provided closure phase and show temporal variations and asymmetries in the surrounding dust, with a difference of about 15 % in intensity between two sides of the star. Comparison with earlier interferometric measurements showed a substantial reduction in dust surrounding the star over one decade. Interferometric observations of six Mira-type stars: R Aqr, CIT 3, χ Cyg, W Aql, R Leo, and U Ori have been performed by Tatebe et al. (2006) at Infrared Spatial Interferometer (ISI) which was comprised of three telescopes. The deduced one-dimensional images show significant changes in the stars and surrounding dust between the two consecutive years, indicating a non-constant gas emission.

Wittkowski et al. (2007) presented the first multi-epoch study that includes mid-infrared and radio interferometry of the oxygen-rich Mira star S Ori obtained with VLTI/MIDI at four epochs and maser emission obtained with the VLBA at three epochs. They concluded that S Ori shows significant phase-dependences of photospheric radii and dust shell parameters and that the Al_2O_3 dust grains and SiO maser spots form at relatively small $\sim$ 1.8-2.4 photospheric radii. Their results suggest increased mass loss and dust formation close to the surface near the minimum visual phase when Al_2O_3 dust grains are co-located with the molecular gas and the SiO maser shells, and a more expanded dust shell after visual maximum. Ohnaka et al. (2007)

carried out VLTI/MIDI observations of carbon-rich Mira variable V Oph at three different phases with three different baselines using four 8.2 m Unit Telescopes. Their observations and modeling indicate that carbon-rich Miras also have extended layers of polyatomic molecules as previously confirmed in oxygen-rich Miras. The temporal variation of the N-band angular size has been found to be largely governed by the variations of the opacity and the geometrical extension of the C_2H_2 layers and the dust shell, which masks the size variation of the photosphere.

Using a grism at the Keck Interferometer, Eisner et al. (2007a) obtained spectrally dispersed ($R \sim 230$) interferometric measurements of the Mira star R Vir. Their data showed that the measured radius of the emission varies substantially from 2.0 to 2.4 μm and simple models could reproduce these variations using extended molecular layers which absorb stellar radiation and reemit it at longer wavelengths. As they observed spectral regions with and without substantial molecular opacity, they could determine the stellar photospheric radius, uncontaminated by molecular emission. They infer that most of the molecular opacity arises at approximately twice the radius of the stellar photosphere.

Asymmetries and motions in the dust shell surrounding *o* Ceti have been reported by Chandler et al. (2007). The measurements were taken with the ISI, a three-element interferometer operating at 11.15 μm and three years of data permited detection of the movement of dust shells in time. Wittkowski et al. (2008) presented J, H, K spectrally dispersed interferometry of S Ori with a spectral resolution of 35 for the Mira variable S Orionis, with the VLTI/AMBER instrument between 1.29 μm and 2.32 μm. The measured visibility and uniform disc diameter variations with wavelength resemble and generally confirm the predictions by previous dynamic model atmospheres. These size variations with wavelength could be understood as the effects arising from water vapor and CO layers lying above the continuum-forming photosphere.

The sizes and shapes of the stars *o* Ceti and R Leonis have been measured in the mid-infrared by Tatebe et al. (2008) using the ISI instrument. The star *o* Ceti appeared to be rather symmetric while the shape of the R Leonis appeared more consistent with a uniform disc plus a point source. Pluzhnik et al. (2009) presented the results of long baseline interferometric observations of the Mira-type star U Ori at 1.51 μm (H_2O band), 1.64 μm (pseudo-continuum), and 1.78 μm (H_2O band), using the three-element IOTA interferometer. They performed model-independent image reconstruction of the envelope around the star using measured visibilities and closure phases. The images show asymmetric structure of the U Ori envelope (Fig. 11), and they discussed the geometric and kinematic structure of the envelope based on a model of an almost face-on expanding and rotating disc around the star.

Le Bouquin et al. (2009a) obtained single-epoch interferometric observations of T Lep with a continuous dataset in the spectral domain (λ =1.5-2.4 μm) and in the spatial domain (interferometric baselines ranging from 11 to 96 m), and they performed a model independent image reconstruction for each spectral bin. Reconstructed images (Fig. 12) confirm the general picture of a central star partially obscured by the surrounding molecular shell of changing opacity. At 1.7 μm, the shell becomes optically thin, with corresponding emission appearing as a ring circling the star. This was the first direct evidence of the spherical morphology of the molecular shell in Mira stars while model fitting confirmed a spherical layer of constant size and changing opacity over the wavelengths.

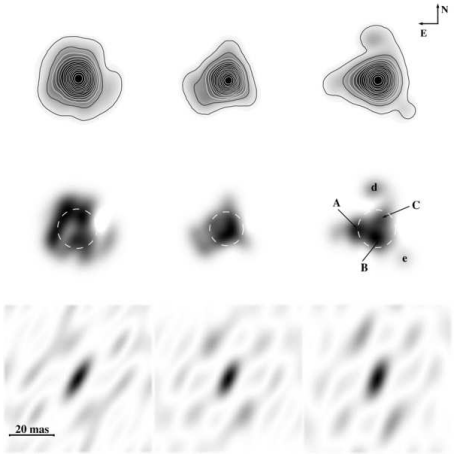

Fig. 11. *Reconstructed images of U Ori. Images are reconstructed at 1.51 μm, 1.64 μm, and 1.78 μm (top, from left to right). The corresponding images of the envelope, obtained by removing the model of the central source are shown in the second row. The bright spots A, B, and C correspond to H_2O maser features. The synthesized beams of the interferometer for all wavelengths are shown at the bottom.*

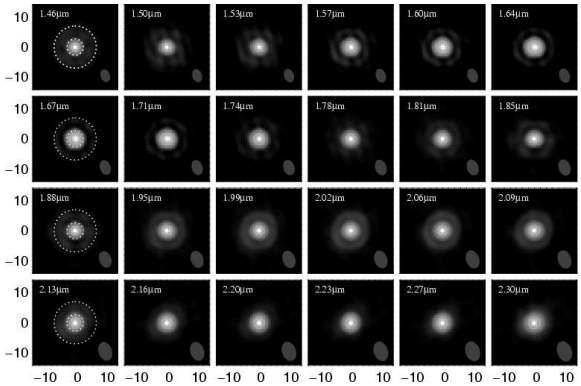

Fig. 12. *Reconstructed images of T Lep. Images are shown for several AMBER spectral bins across the H and K bands. The interferometric beam size is displayed at the bottom-right part of each image. Spatial scale is in mas.*

Lacour et al. (2009) presented infrared interferometric imaging of the S-type Mira star χ Cygni. The star was observed at four different epochs with the IOTA interferometer (H band) using the integrated optics recombiner IONIC. Images show up to 40 % variation in the stellar diameter, as well as significant changes in the limb darkening and stellar inhomogeneities. The model fitting gave precise time-dependent values of the stellar diameter, and reveals presence and displacement of a warm molecular layer. The constant acceleration of the CO molecules during 80 % of the pulsation cycle lead to argument for a free-falling layer.

In order to explore the photosphere of the very cool late-type star VX Sgr and, in particular, the characterization of molecular layers above the continuum forming photosphere, Chiavassa et al. (2010) obtained interferometric observations with the VLTI/AMBER instrument. Reconstructed images and visibilities showed a strong wavelength dependence and the H-band images displayed two bright spots whose positions were confirmed by the geometrical model.

9. PLANETARY NEBULAE

After having been extensively studied in the visible, the Planetary Nebulae and among them the youngest and more dusty ones are now studied in the near and mid-infrared. It is commonly accepted that discs surrounding the central star can be an essential ingredient to the shaping of planetary nebulae, but the spatial resolution of single aperture astronomical instruments is usually not sufficient for detecting and studying these discs. The geometry of the disc and the mass stored are the key parameters for constraining the models of nebula formation, and for tracing back the evolution of the central star. The disc inner edge, as seen from the star, could be thick and dense enough to collimate stellar winds into lobes and knowing its geometry it enables us to better understand the distribution of illuminated and shadowed regions in the extended nebula. The significant progress for these studies has been achieved with the VLT Interferometer and its two instruments: AMBER operating in the near-infrared and MIDI in the mid-infrared providing a typical spatial resolution of 2 and 10 mas, respectively, which is well suited for the study of many aspects of the late evolution of stars and in particular, to deal with the asymmetry in the Planetary Nebula, back to the AGB stars.

Chesneau et al. (2006) presented high spatial resolution observations of the dusty core of CPD-56 8032, taken with the mid-infrared interferometer VLTI/MIDI. The infrared core was almost fully resolved with the three baselines and the signal is interpreted in terms of a ring structure which would define the bright inner rim of the equatorial disc. Geometric models allowed derivation of the main geometrical parameters of the disc, showing that the disc is mostly optically thin in the N band and highly flared. Lagadec et al. (2006) reported on infrared observations of the planetary nebula Hen 2-113 obtained with the same instrument. No clear core at 8.7 μm and no fringes through the N band could be detected and a qualitative interpretation of the object structure is proposed by using a diabolo-like geometrical model. In order to obtain a high spatial resolution information on the dusty core of bipolar planetary nebulae and to directly constrain the shaping process, Chesneau et al. (2007a) obtained observations of the dusty core of the extreme bipolar planetary Ant nebula (Mz 3, Hen 2-154) taken with the VLTI/MIDI. The core was clearly resolved and they suggest an edge-on disc whose major axis is perpendicular to the axis of the bipolar lobes for which they deduce inclination and position angle.

With the purpose of studying the structure of the nebula around the post AGB, the binary star 89 Her, Bujarrabal et al. (2007) obtained N-band interferometric data on the extent of the hot dust emission obtained with the VLTI/MIDI instrument and the IRAM Plateau de Bure Interferometer (PdBI) observations of the ^{12}CO(1-0) and ^{12}CO(2-1) lines and continuum emission. They presented high-resolution PdBI maps, and derived the properties of the nebula from model fitting. Two nebular components are found: an extended hour-glass-like structure and an unresolved very compact component, smaller than 0.4 arcsec. Assuming that the compact component is a Keplerian disc, they derive disc properties that are compatible with expectations for such a structure; in particular, the size of the rotating gas disc that is very similar to the extent of the hot dust component from VLTI data. Assuming that the equator of the extended nebula coincides with the binary orbital plane, they provide new results on the companion star mass and orbit. In order to probe the innermost region of the circumstellar dust shell of the deeply embedded Wolf Rayet star WR 118, Millour et al. (2009a) carried out spectro-interferometric observations using the VLTI/AMBER instrument in the low-spectral resolution mode (R=35). The K-band observations were obtained with three 1.8 m telescopes spanning projected baselines between up to 40 m which allowed them to conclude that WR 118 possibly harbors a pinwheel nebula, suggesting a binary nature of the system.

10. LUMINOUS BLUE VARIABLES: η Carinae

The bright star η Carinae is the most massive and luminous star in our region of the Milky Way. Though it has been extensively studied using many different techniques, its physical nature and the mechanism that led to the creation of the Homunculus nebula are still debated. Van Boekel et al. (2003) presented new high angular resolution observations at near-IR wavelengths of the core of the nebula by using the VLTI/VINCI instrument. The observations provided spatial information on a scale of 11 AU at the distance of η Carinae and the data show that the object is elongated with a de-projected axis ratio of approximately 1.5 and that the major axis is aligned with that of the nebula. The most

likely explanation for this observation was a model in which stellar rotation near the critical velocity causes enhanced mass loss along the rotation axis resulting from the large temperature difference between the pole and equator in rapidly rotating stars. They conclude that η Carinae must rotate in excess of 90% of its critical velocity to account for the observed shape and that the large outburst may have been shaped in a similar way.

To constrain spatially and spectrally the warm dusty environment and the central object, Chesneau et al. (2005b) observed the core of the nebula surrounding η Carinae with the interferometer VLTI/MIDI. In particular, narrow-band images at 3.74 μm and 4.05 μm reveal the butterfly shaped dusty environment close to the central star with unprecedented (sub-arcsecond) spatial resolution (Fig. 13). A void whose radius corresponds to the expected sublimation radius has been discovered around the central source.

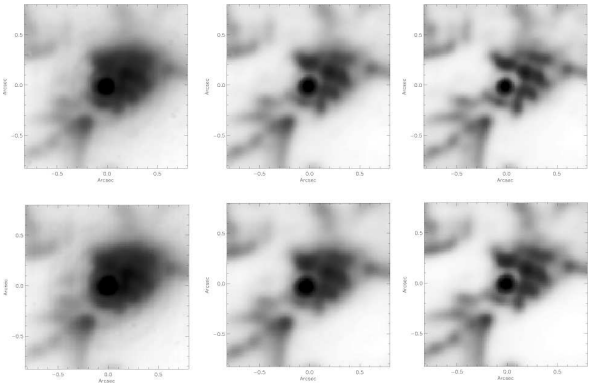

Fig. 13. *The butterfly shaped dusty environment close to η Car. Zoom into the deconvolved images from the 3.74 μm (top) and 4.05 μm (bottom) filters. The raw images are shown on the left side, the deconvolved images at iteration 10 and 40 are shown on the middle and on the right side.*

To study the wavelength dependence of the η Carinae optically thick wind region with a high spatial resolution of 5 mas (11 AU), Weigelt et al. (2007) presented the first NIR spectro-interferometry of the star. The analysis has been performed on the VLTI/AMBER spectrally dispersed interferograms (spectral resolutions of 1500 in the medium spectral resolution mode and 12000 in the high resolution mode) which allowed the investigation of the wavelength dependence of the visibility, differential phase, and closure phase. For the interpretation of the non-zero differential and closure phases measured within the Brγ line, they present a simple geometric model of an inclined, latitude-dependent wind zone. Their observations supported theoretical models of anisotropic winds from fast-rotating, luminous hot stars with enhanced high-velocity mass loss near the polar regions.

With the purpose of resolving the central engine of the η Carinae complex in the near-infrared on angular scales of a few milli-arcseconds, Kervella (2007) used the VLTI/VINCI data in the K band obtained with either two 0.35 m siderostats or two 8-m Unit Telescopes. He reported visibility measurements in satisfactory agreement with the previous results obtained with VLTI/AMBER.

Aiming to constrain the rotational velocity of the primary star and to probe the influence of the companion, Groh et al. (2010) analyzed K-band continuum visibilities from VLTI/VINCI and closure phase measurements from VLTI/AMBER. They conclude that the density structure of the primary wind can be sufficiently disturbed by the companion, thus mimicking the effects of fast rotation, and therefore the fast rotation may not be the only explanation for the interferometric observations.

11. NOVAE

The high spatial resolution studies of Novae in the optical domain has been recently stimulated by emergence of large optical interferometers. Particularly, the outburst that occurred on February 12, 2006 on recurrent nova RS Oph has been extensively observed by different interferometers. Following the outburst, Monnier et al. (2006a) measured its near-infrared size using the IOTA, Keck, and PTI interferometers at multiple epochs. They concluded that the characteristic size of ~ 3 mas hardly changed over the first 60 days of the outburst, ruling out popular models where the near-infrared emission arises from hot gas in the expanding shock. The emission was also found to be significantly asymmetric, evidenced by nonzero closure phases detected by IOTA. Using the PTI interferometer, Lane et al. (2007) performed observations of RS Oph, resolving the emission from the nova for several weeks after the outburst. They reported that the near-IR source which initially expanded to a size of ~ 5 mas, began to shrink around day 10, and reached ~ 2 mas by day 100. They argue that the fact that the emission region appears to shrink does not necessarily imply that the material is falling; what one can see is the effective photospheric diameter, which is a function of the density of the material, and if the mass-loss rate from the central white dwarf drops, the apparent photospheric radius would be expected to shrink even as the material continues flowing outward.

Chesneau et al. (2007b) reported on spectrally dispersed VLTI/AMBER observations of RS Oph five days after the discovery of the outburst. Using three baselines and a spectral resolution of R=1500, they measured the extension of the milliarcsecond scale emission in the K band continuum and in the Brγ and He I 2.06 μm lines, which allowed to get an insight into the kinematics of the line forming regions. Their results confirm the basic fireball model (Fig. 14), contrary to the conclusions of other interferometric observations conducted by Monnier et al. (2006a). Barry et al. (2008) reported N-band (8 to 12.5 μ) observations of RS Oph using the Keck Interferometer 3.8 days following the outburst. The data show evidence of enhanced neutral atomic hydrogen emission and atomic metals includ-

ing silicon located in the inner spatial regime near the white dwarf. They report also nebular emission lines and evidence of hot silicate dust in the outer spatial region, centered at $\sim$ 17 AU from the white dwarf, which were not found in the inner regime. Their results support a model in which the dust appears to be present between outbursts and is not created during the outburst event.

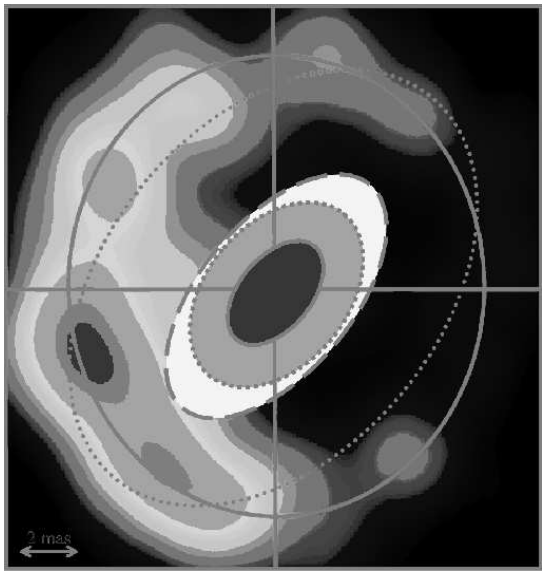

Fig. 14. *RS Oph outburst. Sketch of the near-IR ellipses extensions compared with the radio structure observed at t= 13.8d (thick extended ring, O'Brien et al. 2006). The continuum ellipse is delimited by the solid line, the ellipse that corresponds to the core of Brγ by the dotted line and the one corresponding to the core of HeI by the dashed line. The small dotted line delimits the Brγ ellipse scaled at t= 13.8 d. North is up, east left.*

Lane et al. (2007) have resolved the classical nova V1663 Aql using a long-baseline near-IR interferometry from the PTI interferometer covering the period from $\sim$ 5 to 18 days after the peak brightness. They directly measured the shape and size of the fireball, (which they found to be asymmetric) and the apparent expansion rate. Assuming a linear expansion model, the time of the initial outburst approximately 4 days prior to the peak brightness was infered. In order to improve the distance determination and to constrain the mechanisms leading to very efficient dust formation under the physical conditions encountered in novae ejecta, Chesneau et al. (2008) presented the first high spatial-resolution monitoring of the dust-forming nova V1280 Sco. Spectra and visibilities were regularly acquired between the onset of dust formation, 23 days after the discovery (11 days after the maximum), using the beam-recombiner instruments AMBER (near-IR) and MIDI (mid-IR). These observations allowed determination of the apparent linear expansion rate for the dust shell 0.35 $\pm$ 0.03 mas day, and the approximate ejection time of the matter in which dust formed (t_{ejec} = 10.5$\pm$ 7 d), i.e. close to the maximum brightness.

Chesneau et al. (2011) reported on near-IR interferometric observations of the recent 2011 outburst of the recurrent nova T Pyx. They obtained near-IR observations of T Pyx at dates ranging from 2.4 to 48.2 days after the outburst with the CLASSIC recombiner located at the CHARA array and with the PIONIER and AMBER recombiners located at the VLTI array. Comparing expansion of the H and K band continua as well as the Brγ emission line, and infering information on the kinematics and morphology of the early ejecta, they concluded that it could be most simply interpreted within the frame of a bipolar model oriented nearly face-on.

12. YOUNG STELLAR OBJECTS

The very close environments of young stars are the hosts of fundamental physical processes such as star-disc interactions, mass accretion, and ejection. The extraordinary interest in the inner region of a circumstellar disc results from the assumption that the formation of planets is favored there, focusing on how accretion discs evolve into protoplanetary discs and, finally, to debris discs and planets. Optical interferometry is playing an important role in elucidating the earliest stages of planetary formation by probing the density and temperature structure of the discs presumably before the planet formation. The first successful observation of a Young Stellar Objects (YSOs) with stellar interferometry was reported by Malbet et al. (1998) who resolved the young outbursting star FU Ori using a 100-m long baseline in the K band with the PTI. Using the IOTA interferometer Millan-Gabet et al. (1999) resolved the Herbig Ae/Be star AB Aur, finding the near-IR emission to be much larger than expected.

Radically improved infrared detectors have recently allowed optical interferometers to investigate the inner accretion discs around young stellar objects (Millan-Gabet et al. 2001, Akeson et al. 2000, 2002, Tuthill et al. 2001, Danchi et al. 2001). In most cases, the near-IR sizes were found to be significantly larger than expected from the favored disc models of the time (Malbet and Bertout 1991). The complex morphological structure of these environments has been confirmed by the now quite rich data sets obtained by near-infrared long-baseline interferometry. While observations in millimeter range probe cooler outer disc regions and layers close to the midplane of circumstellar discs, observations in the mid-infrared wavelength regime are more sensitive to warmer disc arreas, such as the surface of the inner regions where the dust is directly irradiated by the central star.

12.1. Herbig Ae/Be stars

Pre-main sequence stars in the intermediate mass range (1.5-3 $M_{\odot}$), called Herbig Ae and Be stars, are observed to be surrounded by circumstellar material which reveals itself by discrete emission

lines and by continuous excess emission in spectral energy distribution (SED). The spatial distribution of this material however has been subject to debate: both geometrically flat disc models and spherically symmetric envelope models can reproduce the observed SED. Unveiling the structure of the discs is essential for our understanding of the star and planet formation process. In particular, models predict that in the innermost AU around the star, the dust disc forms a "puffed-up" inner rim (Dullemond et al. 2001), which should result in a strongly asymmetric brightness distribution for discs seen under intermediate inclination.

The Herbig Ae/Be star LkH α 101 has been imaged with high angular resolution at a number of wavelengths in the near-infrared (from 1 to ~ 3 μm), using the Keck I Telescope, and also observed in the mid-infrared (11.15 μm) by Tuthill et al. (2002) using the ISI instrument. The resolution of the LkH α 101 disc by ISI mid-infrared interferometry constitutes the first such measurement of a young stellar object in this wavelength region, and the resolved circular disc with a central hole or cavity (Fig. 15) reported by Tuthill et al. (2001) has been confirmed by this study.

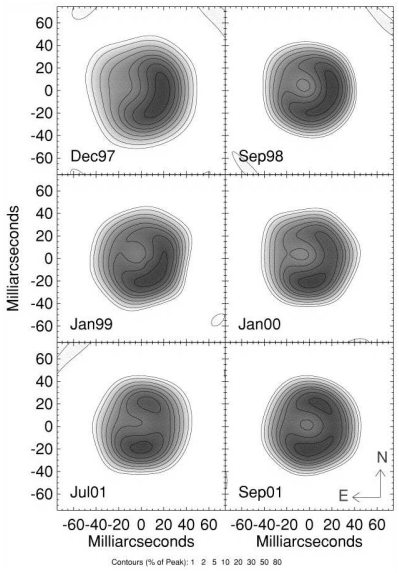

Fig. 15. *K-band images of the resolved disc of Herbig Ae/Be star LkHα 101. The images are reconstructed from data taken at six different epochs.*

Eisner al. (2003) have observed the Herbig Ae/Be sources AB Aur, VV Ser, V1685 Cyg (BD +40°4124), AS 442, and MWC 1080 with the PTI, obtaining the near-IR interferometric observations which allowed them to determine the angular size scales and orientations predicted by uniform-disc and showing the evidence for significantly inclined morphologies. The long baseline mid-infrared interferometric observations of the circumstellar discs surrounding Herbig Ae/Be stars have also been performed by Leinert et al. (2004), using the VLTI/MIDI instrument. They observed seven nearby Herbig Ae/Be stars and resolved all objects in the wavelength range from 8 μm to 13.5 μm, with a spectral resolution of 30. Characteristic dimensions of the emitting regions at 10 μm were found to be from 1 to 10 AU.

Eisner et al. (2004) have observed 14 Herbig Ae/Be sources with the long- baseline near-infrared Palomar Testbed Interferometer (PTI). They determined the size scales and orientations of the 2.2 μm emission, being able to place firm constraints on the inclinations of most sources; seven objects displayed significantly inclined morphologies. The inner disc inclinations derived from their data are generally compatible with the outer disc geometries inferred from millimeter interferometric observations, implying that Herbig Ae/Be stellar discs are not significantly warped. Monnier et al. (2005a,b) reported the results of a sensitive K-band survey of Herbig Ae/Be disc sizes using the Keck Interferometer. Targets were chosen to span the maximum range of stellar properties to probe the disc size dependence on luminosity and effective temperature. For most targets, the measured near-infrared sizes (ranging from 0.2 to 4 AU) support a simple disc model possessing a central optically thin (dust-free) cavity, ringed by hot dust emitting at the sublimation temperatures.

Preibisch et al. (2006) used the mid-infrared long-baseline interferometry to resolve the circumstellar material around the Herbig Ae star HR 5999, providing the first direct measurement of its angular size and deriving the constraints on the spatial distribution of the dust. MIDI at the VLTI was used to obtain a set of spectrally dispersed (R$\simeq$ 30) interferometric measurements of the star at different projected baseline lengths and position angles. A satisfactory fit to the observed visibilities was found with a model of a geometrically thin disc that is truncated at 2.6 AU and seen under an inclination angle of 58°.

The first closure-phase measurements in the near-infrared obtained on a young stellar object were made by Millan-Gabet et al. (2006a) using the three-telescope long-baseline interferometer IOTA. They reported on the detection of localized off-center emission at 1-4 AU range in the circumstellar environment of the AB Aur. When probing sub-AU scales, all closure phases were close to zero degrees, as it was expected given the previously determined size of the AB Aurigae inner-dust disc. However, a clear non-zero closure-phase signal was detected on one triangle containing relatively short baselines, requiring a high degree of non-point symmetry from emission at larger scales in the disc. Using the same interferometer, Monnier et al. (2006b) reported results from the near-infrared (λ =1.65 μm) closure-phase survey of YSOs. These closure phases allowed them to unambiguously detect departures from central symmetry in the emission pattern from YSO discs on the scale of $\sim$ 4 mas as expected from generic "flared disc" models. Their data support disc models with curved inner rims because the expected emission appears symmetrically distributed around the star over a wide range of inclination angles. In contrast, their results are incompatible with the models possessing vertical inner walls, which predict large closure

phases from the near-infrared disc emission, that is not seen in their data.

Tatulli et al. (2007) investigated the origin of the Brγ emission of the Herbig Ae star HD 104237 on AU scales, using VLTI/AMBER at a spectral resolution R=1500, and spatially resolving the emission in both the Brγ line and the adjacent continuum. Assuming that the K-band continuum excess originates in a "puffed-up" inner rim of the circumstellar disc, they discussed the likely origin of Brγ concluding that this emission most likely arises from a compact disc wind launched from a region 0.2-0.5 AU from the star with a spatial extent similar to that of the near infrared continuum emission region, i.e. very close to the inner rim location. Eisner et al. (2007b) used spectrally dispersed near-IR interferometry PTI data to constrain the temperature profiles of sub-AU sized regions of 11 Herbig Ae/Be sources. They find that a single-temperature ring does not reproduce well the data; rather the models incorporating radial temperature gradients are preferred. They speculate that these gradients may arise in a dusty disc, or may reflect separate gas and dust components with arises from hot circumstellar dust and gas in sub-AU sized disc.

The young stellar object MWC 297, observed with the VLT interferometer equipped with the AMBER instrument, has been spatially well resolved in the continua as in the Brγ emission line (Malbet et al. 2007). The change in the visibility with wavelength could be interpreted by the presence of an optically thick disc responsible for the visibility in the continuum and of a stellar wind traced by the Brγ emission line. The disc and wind models yielded a consistent inclination of the system of approximately 20°. A picture emerged in which MWC 297 is surrounded by an equatorial flat disc (Fig. 16) that is possibly still accreting and an outflowing wind that has a much higher velocity in the polar region than at the equator.

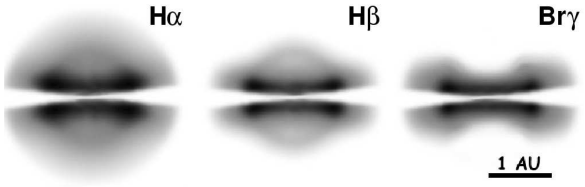

Fig. 16. *MWC 297 edge-on intensity maps of the wind. Maps are presented in the Hα, Hβ, Hγ lines.*

Using the sub-milli-arcsecond near-infrared CHARA interferometry, Tannirkulam et al. (2008a) have detected a strong emission from inside the dust destruction radius of Herbig Ae stars MWC 275 and AB Aur. Their sub-milli-arcsecond resolution observations unambiguously place the emission between the dust destruction radius and the magnetospheric corotation radius. They argue that this new component corresponds to a hot gas inside the dust sublimation radius, confirming previous claims based on spectrally resolved interferometry and dust evaporation modeling. Tannirkulam et al. (2008b) presented comprehensive models for these two stars, aiming to explain their spectral energy distribution (from UV to millimeter) and long-baseline interferometry (from near-infrared to millimeter) simultaneously, by using data from the literature combined with mid-infrared data from the Keck interferometer. To fit the near infrared spectral energy distribution and long-baseline sub-milli-arcsecond near-infrared CHARA observations, they include an additional gas emission component with a similar size scale to the dust rim inside the sublimation radius. In the absence of shielding of starlight by gas, they show that the gas-dust transition region in these YSOs should contain highly refractory dust, sublimating at $\sim$ 1850 K.

Soon after, the morphology of the protoplanetary disc surrounding the Herbig Ae star AB Aur has been derived by di Folco et al. (2009) using the N-band observations at VLTI/MIDI. To derive the key constraints on the launching point of the jets and on the geometry of the winds in AB Aur, Rousselet-Perraut et al. (2010) used the visible spectro-polarimeter VEGA installed on the CHARA optical array which could efficiently probe the structure and the kinematics of the hot circumstellar gas at sub-AU scales. They resolved AB Aur in the Hα line and in a part of the continuum even at the smallest baseline of 34 m. The small P-Cygni absorption feature is indicative of an outflow but could not be explained by a spherical stellar wind model, instead it favors a magneto-centrifugal disc or disc-wind geometry.

Using the VLTI/AMBER instrument, Kraus et al. (2008a) resolved spatially and spectrally (R = 1500) the inner (< 5 AU) environment of five Herbig Ae/Be stars (HD 163296, HD 104237, HD 98922, MWC 297, V921 Sco) in the Brγ emission line as well as in the adjacent continuum. From the measured wavelength-dependent visibilities, they derived the characteristic size of the continuum and Brγ line-emitting region. Kraus et al. (2008b) studied the geometry and the physical conditions in the inner circumstellar region around the young Herbig Be star MWC 147 using the long-baseline IOTA/FLOUR spectro-interferometry in the near-infrared K and H-bands VLTI/AMBER observations, PTI archive data, as well as the mid-infrared N-band VLTI/MIDI observations. They conclude that the near-infrared continuum emission from MWC 147 is dominated by accretion luminosity emerging from an optically thick inner gaseous disc while the mid-infrared emission also contains contributions from the outer, irradiated dust disc.

Isella et al. (2008) investigated the origin of the near-infrared emission of the Herbig Ae star MWC 758 on sub-astronomical unit scales using spectrally dispersed low resolution (R = 35) VLTI/AMBER interferometric observations in the H and K bands. They find that the K band visibilities and closure phases are consistent with the presence of a dusty disc inner rim located at the dust evaporation distance (0.4 AU) while the bulk of the H-band emission arises within 0.1 AU from the central star. Comparing the observational results with theoretical model predictions, they suggest that the H band emission is dominated by a hot gaseous accretion disc.

Ragland et al. (2009) presented spatially resolved K- and L-band spectra (at spectral resolutions R = 230 and R = 60 respectively) of MWC 419, obtained with a configuration of the 85 m baseline Keck Interferometer. Their observations being sensitive to the radial temperature distribution in the inner region of the disc allowed to fit the visibility data with a model having a power-law temperature gradient. The slope of the power law is close to that expected from an optically thick disc, and the measured disc size at Brγ spectral line suggests that emitting hydrogen gas is located inside (or within the inner regions) of the dust disc. Using the VLTI/AMBER, Kraus et al. (2009) obtained near-infrared (H- and K-band) spectro- interferometric data on R CrA, observing with three telescopes in a linear array configuration which provided direct information on the radial intensity profile. In addition, the observations covered a wide position angle range, also probing the position angle dependence of the source brightness distribution. Detecting, for the first time, strong non-localized asymmetries in the inner regions of a Herbig Ae disc, their study supports the existence of a puffed-up inner rim in YSO discs.

Renard et al. (2010) gathered interferometric measurements for the young star HD 163296 with various interferometers (VLTI, IOTA, KeckI and CHARA) allowing a model independent image to be reconstructed (Fig. 17). The obtained H and K-band images of the stellar surroundings detect several significant features that they relate to an inclined asymmetric flared disc around the star. These images confirmed that the morphology of the close environment of young stars is more complex than the simple models previously used.

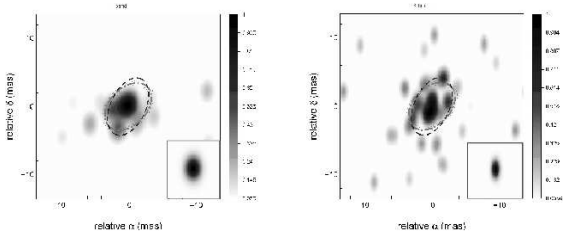

Fig. 17. *Reconstructed images of HD163296. Images obtained in the H (left) and K bands (right), after a convolution with a Gaussian beam at the interferometer resolution (sub-panel in the right corner of each plot).*

Benisty et al. (2010) presented new long-baseline spectro-interferometric observations of the Herbig Ae star HD 163296 obtained in the H and K bands with the AMBER instrument at the VLTI. They presented the most comprehensive (u,v) coverage achieved so far for a young star. The circumstellar material was resolved at the sub-AU spatial scale and closure phase measurements indicated a small but significant deviation from point-symmetry. A successful fit to the spectral energy distribution, near-infrared visibilities and closure phases was found with a model in which the dominant contribution to the H and K band emission originates in an optically thin, smooth and point-symmetric region extending from about 0.1 to 0.45 AU, where at a distance of 0.45 AU from the star, silicates condense, the disc becomes optically thick and develops a puffed-up rim whose skewed emission can account for the observed non-zero closure phases.

12.2. T Tauri stars

T Tauri stars are low-mass ($\sim$ 2 $M_\odot$) pre-main-sequence objects, thought to be early analogs of stars like our own Sun. A wealth of evidence, including direct imaging at millimeter and optical wavelengths and modeling of spectral energy distributions, has confirmed the long-espoused hypothesis that T Tauri stars are surrounded by massive discs of dust and gas. Moreover, observed line profiles and UV continuum excesses indicate that T Tauri stars are actively accreting material from their circumstellar discs. The structure of the innermost disc regions may reveal the mechanism by which material is accreted through the disc onto the star. In the current paradigm, T Tauri discs are truncated by the stellar magnetosphere within the corotation radius, with material accreting along magnetic field lines onto high-latituderegions of the star. For typical T Tauri stellar masses, radii, magnetic field strengths, and accretion rates, predicted truncation radii range from 0.02 to 0.2 AU and observational measurements of these truncation radii are an obviously important test of the theory of magnetospheric accretion.

Currently, only near-IR interferometric observations have sufficient spatial resolution to probe directly the geometry and temperature of hot (1000-2000 K) disc regions within 1 AU of young stars. Observations of the inner discs of a few of the brightest T Tauri stars (Akeson et al. 2000, Colavita et al. 2003) demonstrated that inner discs around lower mass stars ($<$ 5 $M_\odot$) are larger than inferred by fitting geometrically thin accretion disc models to SEDs (e.g. Beckwith et al. 1990). Inclusion of puffed-up inner walls in the models leads to consistent fits to both interferometric and spectral energy distribution data for these objects (Eisner et al. 2004, Muzerolle et al. 2003). In order to explore such trends, a larger sample of resolved inner discs of T Tauri stars has been observed. Akeson et al. (2005a) presented observations of four T Tauri stars using long baseline infrared interferometry from the PTI. The target sources, T Tau, SU Aur, RY Tau, and DR Tau, are all known to be surrounded by dusty circumstellar discs. The observations that directly trace the inner regions ($<$1 AU) of the disc have been used to constrain the physical properties of this material. The main conclusion of their modeling is that emission from inner gas discs (between the magnetic truncation radius and the dust destruction radius) can be a significant component in the inner disc flux for sources with large inner dust radii.

Generally, T Tauri stars are faint objects and the significant progress has been achieved by utilizing the two 10 m Keck telescopes interferometer: Colavita et al. (2003) presented observations of the T Tauri object DG Tau for which the resolved com-

ponent has a radius of 0.12-0.24 AU depending on the assumed stellar and extended component fluxes as well as the model geometry used. Eisner et al. (2005) determined inner disc sizes and temperatures for four solar-type (1-2 $M_\odot$) classical T Tauri stars, AS 207A, V2508 Oph, AS 205A, and PX Vul. In addition to interferometry, the spectroscopic and photometric data provided estimates of stellar properties, mass accretion rates, and disc corotation radii. Models incorporating puffed-up inner disc walls generally provided better fits to the data than geometrically flat accretion disc models with inner holes, similar to previous results for higher mass Herbig Ae stars. The measured inner disc sizes are larger than disc truncation radii predicted by magnetospheric accretion models, with larger discrepancies for sources with higher mass accretion rates. They suggest that the measured sizes correspond to dust sublimation radii, and that optically thin gaseous material may extend further inward to the magnetospheric truncation radii. The deduced inner disc measurements constrain the location of terrestrial planet formation as well as potential mechanisms for halting giant planet migration. Akeson et al. (2005b) presented observations of the T Tauri stars BP Tau, DG Tau, DI Tau, GM Aur, LkCa 15, RW Aur, and V830 Tau, also using the long baseline infrared interferometry at K band (2.2 μm) from the Keck Interferometer. Assuming that the K-band-resolved emission traces the inner edge of the dust disc, they compare the measured characteristic sizes to predicted dust sublimation radii and find that the models require a wide range of dust sublimation temperatures and possibly optical depths within the inner rim to match the measured radii. Eisner et al. (2007c) presented observations of a sample of 11 solar-type T Tauri stars in nine systems. They use these observations to probe the circumstellar material within 1 AU, measuring the circumstellar-to-stellar flux ratios and angular size scales of the 2.2 μm emission. Their sample spans a range of stellar luminosities and mass accretion rates, allowing investigation of potential correlations between inner disc properties and stellar or accretion disc properties. They suggest that the mechanism by which the dusty inner disc is truncated may depend on the accretion rate of the source; in objects with low accretion rates, the stellar magnetospheres may truncate the discs, while sublimation may truncate dusty discs around sources with higher accretion rates.

Ratzka et al. (2007) used interferometric observations in the N-band obtained with the VLTI/MIDI instrument, together with 10 μm spectra recorded by the infrared satellite Spitzer in order to improve knowledge of the structure of the inner few AU of the circumstellar disc around the nearby T Tauri star TW Hya. They found that the most of the observed crystalline material is in the inner, unresolved part of the disc, about 1 AU in radius. They proposed a geometry of the inner disc where an inner hole still exists but at a much reduced radius with the transition from zero to full disc height between 0.5 and 0.8 AU, and with an optically thin distribution of dust inside. With the same instrument, the study of the inner region ($\sim$ 1.0 AU up to a few 10 AUs) of the circumstellar disc around the typical T Tauri star RY Tau has been made by Schegerer et al. (2008). They show that a modestly flaring disc model with accretion can explain both the observed spectral energy distribution and the mid-infrared visibilities obtained with MIDI. From the study of the silicate emission feature they see evidence for dust evolution, with a decreasing fraction of small amorphous and an increasing fraction of crystalline particles closer to the star.

Eisner et al. (2009) presented spatially resolved near-IR spectroscopic observations of 15 young stars. Using a grism spectrometer behind the Keck interferometer, they obtained an angular resolution of a few milli-arcseconds, enabling probes of both gas and dust in the inner discs surrounding the target stars. They find that the angular size of the near-IR emission typically increases with wavelength, indicating hot, presumably gaseous material within the dust sublimation radius. Their data also clearly indicate Brγ emission arising from hot hydrogen gas, suggesting the presence of water vapor and carbon monoxide gas in the inner discs of several objects, and showing that the gaseous emission was more compact than the dust continuum emission in all cases.

12.3. FU Orionis stars

Following the first observations (Malbet et al. 1998), Malbet et al. (2005) reported new near-infrared, long-baseline interferometric observations at the AU scale of the pre-main-sequence star FU Orionis with the PTI, IOTA and VLTI interferometers. This young stellar object was observed over a period of 6 years from 1998 to 2003. Their data resolved FU Ori at the AU scale, and provided new constraints at shorter baselines and shorter wavelengths. Their extensive (u, v)-plane coverage, coupled with the published spectral energy distribution data, allowed to test the accretion disc scenario. They find that the most probable explanation for these observations is that FU Ori hosts an active accretion disc for which they constrain the geometry, including inclination and a position angle (Fig. 18). In addition, a 10% peak-to-peak oscillation was marginally detected in the data from the longest baselines, which they interpret as a possible disc hotspot or companion.

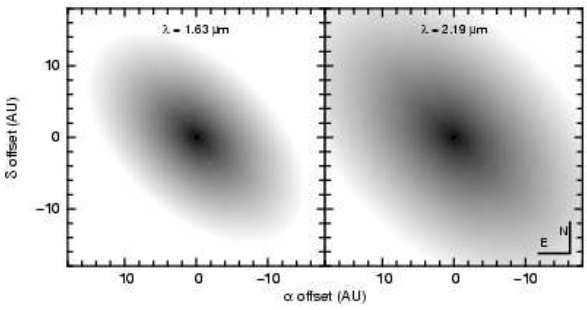

Fig. 18. *Synthetic images of FU Ori. Accretion disc model in H (left) and K (right). Images are in logarithmic scale.*

Millan-Gabet et al. (2006b) presented new K-band long-baseline Keck Interferometer observations of three young stellar objects of the FU Orionis class, namely V1057 Cyg, V1515 Cyg, and Z CMa-SE. The interferometer clearly resolves the source of near-infrared emission in all three objects. Using simple geometric models, they derive size scales (0.5-4.5 AU) for this emission. All three objects appear significantly more resolved than expected from simple models of accretion discs tuned to fit the broadband optical and infrared spectrophotometry. They hypothesize that the large-scale emission (tens of AU) in the interferometer field of view is responsible for the surprisingly low visibilities and they argue that this emission may arise in scattering by large envelopes believed to surround these objects.

12.4. Massive Young Stellar Objects

Massive Young Stellar Objects (MUSOs) are luminous, embedded infrared sources that show many signs that they are still actively accreting mass. Their luminosity is such that they are expected to be ionizing their surroundings to produce an HII region, and most of them appear to be driving bipolar molecular flows. The sub-millimeter interferometry is beginning to reveal evidence of rotating, disc-like structures on scales of hundreds of AU. There is great interest in knowing the distribution of the infalling and outflowing material on smaller scales; this distribution may provide clues to which physical processes are controlling the dynamics and setting the final mass of the star. The mid-IR (8-13 m) emission from MYSOs is thought to arise in the warm (∼300 K) dust in the envelope heated by the young star. Previous modeling (e.g. Churchwell et al. 1990) has indicated that the size of the mid-IR emission region should be unresolved at the typical distances of MYSOs by single-dish telescopes, and this was borne out by observations (Kraemer et al. 2001, Mottram et al. 2007). Due to the small angular extent of MYSOs, one needs to overcome the limitations of conventional thermal infrared imaging regarding the spatial resolution in order to get observational access to the inner structure of these objects. Very few massive young stellar objects (MYSO) have been studied in the infrared at high angular resolution due to their rarity and large associated extinction.

Attempting to overcome the spatial resolution limitations of conventional thermal infrared imaging, de Wit et al. (2007) reported on mid-infrared resolved interferometric observations with VLTI/MIDI of the massive young stellar object W33A. The spectrally dispersed visibilities indicate that W33A has a size of approximately 120 AU (0.030 arcsec) at 8 μm, that increases to 240 AU at 13 μm, (scales previously unexplored among MYSOs) the observed trend beeing consistent with the temperature falling off with distance. The circumstellar structure on 100 AU scales of W33A has also been probed by de Wit et al. (2010) using the same instrument and proved to be inconsistent with models including a rotationally flattened envelope and outflow cavities. The observations were also compared to models with and without (dusty and gaseous) accretion discs. A satisfactory model was constructed in which the 10 μm emission on 100 AU scales is dominated by the irradiated walls of the cavity sculpted by the outflow. Also they ruled out the presence of dust discs with total (gas and dust) masses more than 0.01 $M_\odot$. Linz et al. (2009) employed the VLTI/MIDI instrument to investigate M8E-IR, a massive young stellar object suspected of containing a circumstellar disc. They resolve the mid-infrared emission of the star and find typical sizes of the emission regions of the order of 45 AU. The data does not provide evidence for an extended circumstellar disc with sizes ≈ 100 AU but requires the presence of an extended envelope. In addition, they present 24.5 μm images that clearly distinguish between M8E-IR and the neighbouring ultracompact H II region and which show the cometary-shaped infrared morphology of the latter source.

Kraus et al. (2010) reported near-infrared interferometric observations that spatially resolve the astronomical unit scale distribution of hot material around IRAS 13481-6124 which harbours a central object of about 20 $M_\odot$, embedded in a cloud with a total gas mass of ∼ 1,5 $M_\odot$. To directly detect this disc and to characterize its inner structure, they used the VLTI/AMBER combining the light of three VLTI 1.8-m telescopes and measuring visibilities and closure phases in 17 spectral channels in the K-band. Complementary VLTI observations with speckle-interferometry from the ESONew Technology Telescope, provided precise spatial information for baseline lengths of less than 3.5 m, and allowed a model independent image reconstruction. This image shows an elongated structure consistent with a disc seen at an inclination angle of ∼ 45°. Using geometric and detailed physical models, they found a radial temperature gradient in the disc, with a dust-free region less than 9.5 AU from the star, qualitatively and quantitatively similar to the discs observed in low-mass star formation. Perpendicular to the disc plane they observed a molecular outflow and two bow shocks, indicating that a bipolar outflow emanates from the inner regions of the system.

Follert et al. (2010) employed mid-infrared interferometry, using the VLTI/MIDI, to investigate the Kleinmann-Wright Object. A qualitative analysis of the data indicated a non-rotationally symmetric structure, e.g. the projection of an inclined disc. Their analysis suggests the existence of a circumstellar disc of 0.1 $M_\odot$ at an intermediate inclination, while an additional dusty envelope was not necessary for fitting the data. To investigate the structure of IRS 9A on scales as small as 200 AU, Vehoff et al. (2010) carried out bservations in the N-band with the VLTI/MIDI, providing spatial information on scales of about 25-95 milli-arcseconds, while additional interferometric observations which probe the structure of the object on larger scales were performed with aperture masking at Gemini South telescope. A warm compact unresolved component was detected by MIDI which is possibly associated with the inner regions of a flattened dust distribution; a geometric model consisting of a warm (1000 K) ring (400 AU diameter) and a cool (140 K) large envelope provided a good fit to the data.

13. DEBRIS DISCS

The circumstellar dust around stars with ages above $\sim$ 10 Myr might be partially remnants from the primordial discs. The discs are however mostly thought to be filled up by the populations of planetesimals that were not used to build up planets. These leftovers are supposed to produce dust by mutual collisions or cometary activity. The study of those debris discs provides one of the best means to explore the properties (size, density, orientation) and evolution of planetary systems.

Absil et al. (2006) performed precise K-band visibility measurements of Vega at both short ($\sim$ 30 m) and long ($\sim$ 150 m) baselines at the CHARA Array in order to separately resolve the emissions from the extended debris disc (short baselines) and from the stellar photosphere (long baselines). They show that the presence of a close companion is highly unlikely as well as other possible perturbations (stellar morphology), and deduce that they have most probably detected the presence of dust in the close neighbourhood of Vega. Peterson et al. (2006b) reported optical interferometric observations (the closure phase at the NPOI) showing that Vega has the asymmetric brightness distribution of the bright, slightly offset polar axis of a star rotating at $\sim$90% of its breakup velocity. In addition to explaining the unusual brightness and line shape peculiarities, this result leads to the prediction of an excess of near-infrared emission compared to the visible, in agreement with observations. The large temperature differences predicted across Vega's surface call into question composition determinations, adding uncertainty to star's age and opening the possibility that its debris disc could be substantially older than previously thought. The large temperature variation across Vega's surface has been confirmed by Aufdenberg et al. (2006a,b) using high-precision interferometric measurements of Vega with the CHARA/FLOUR recombiner in the K' band at projected baselines between 100 and 270 m. The measured visibility amplitudes beyond the first lobe are significantly weaker than expected for a slowly rotating star characterized by a single effective temperature and surface gravity. This measurements, when compared to synthetic visibilities and synthetic spectrophotometry from a Roche-von Zeipel gravity-darkened model atmosphere, provided strong evidence for the model of Vega as a rapidly rotating star viewed very nearly pole-on. The best-fitting model indicates that Vega is rotating at $\sim$90% of its angular break-up rate.

As a part of a near-infrared interferometric survey of debris disc stars, di Folco et al. (2007) probed the first 3 AU around τ Ceti and ϵ Eridani with the CHARA array in order to gauge the 2 μm excess flux emanating from possible hot dust grains in the debris discs, and also to resolve the stellar photospheres. The short baseline observations allowed to disentangle the contribution of an extended structure from the photospheric emission, while the long baselines constrained the stellar diameter. They have detected a resolved emission around τ Cet, corresponding to a spatially integrated, fractional excess flux with respect to the photospheric flux around the star, interpreting the photometric excess as a possible signature of hot grains in the inner debris disc. Absil et al. (2008) obtained high-precision interferometric observations in the near-infrared K band with the the CHARA Array, focused on a sample of six bright A and early F-type stars. They confirmed hot debris disc around Vega (Absil et al. 2006) which remains the only secure resolved detection within the context of this survey.

Le Bouquin et al. (2009b) studied the spin-orbit orientation of the Fomalhaut system composed of a central A4V star, a debris disc, and a recently discovered planetary companion. They used a spectrally resolved, near-IR long baseline interferometry to obtain precise measurements across the Brγ absorption line. The achieved astrometric accuracy of $\pm$3 μas and the spectral resolution R=1500 from the VLTI/AMBER instrument allowed to spatially and spectrally resolve the rotating photosphere as well. They find the position angle for the stellar rotation axis to be perpendicular to the measurement for the disc position angle (Fig. 19), validating the standard scenario for the star and planet formation in which the angular momenta of the planetary systems are expected to be colinear with the stellar spins.

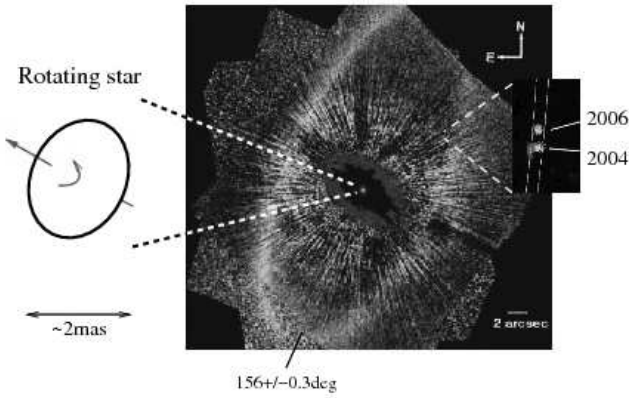

Fig. 19. *Rapidly rotating Fomalhaut and it's debris disc. The signature of the rotating photosphere of Fomalhaut is clearly detected (left) and is compared to the debris disc and the planetary companion (right) imaged in the visible by Kalas et al. (2008).*

14. EXOPLANETS

The detection of close and faint companions is an essential step in many astrophysical fields, including the search for planetary companions. Of the over 450 exoplanets known to date, more than 420 of them have been discovered using radial velocity studies, a method that tells nothing about the inclination of the planetary orbit. Because it is more likely that the companion is a planetary-mass object in a moderate- to high-inclination orbit than a low-mass stellar object in a nearly face-on orbit, the secondary bodies are usually presumed to be pla-

nets. However, interferometric observations allow to inspect the angular diameter fit residuals to calibrated visibilities in order to rule out the possibility of a low-mass stellar companion in a very low-inclination orbit. The first determination of the diameter of an extrasolar planet through purely direct means has been performed by Baines et al. (2007) who measured the angular diameter of the transiting extrasolar planet host star HD 189733 using the CHARA optical/IR interferometric array. Combining their new angular diameter of 0.377 ± 0.024 mas with the Hipparcos parallax leads to a linear radius for the host star of 0.779 ± 0.052 $R_{\odot}$ and a radius for the planet of 1.19 ± 0.08 $R_{\rm Jupiter}$ and providing a mean density of the planet of 0.91 ± 0.18 g cm^{-3}. Baines et al. (2008) observed 22 exoplanet host stars to search for stellar companions in low-inclination orbits that may be masquerading as planetary systems. While no definitive stellar companions were discovered, it was possible to rule out certain secondary spectral types for each exoplanet system observed by studying the errors in the diameter. Baines et al. (2009) directly measured the angular diameters for 11 exoplanet host stars (one dwarf, four subgiants, and six giants) using CHARA interferometer and calculated their linear radii and effective temperatures.

Matter et al. (2010) performed the observation of Gliese 86b which constituted the first attempt at an exoplanet detection with the VLTI instrument MIDI while Baines et al. (2010) used the CHARA interferometer to observe 20 exoplanet host stars and considered five potential secondary spectral types: G5 V, K0 V, K5 V, M0 V, and M5 V. All secondary types could be eliminated from consideration for seven host stars and no secondary stars of any spectral type could be ruled out for seven more. The remaining six host stars showed a range of possible secondary types.

In order to examine astrophysical parameters and habitable zone of the exoplanet hosting Star GJ 581, von Braun et al. (2011a) used long-baseline interferometric measurements from the CHARA Array, coupled with trigonometric parallax information, to directly determine its physical radius, while photometry data were used to perform spectral energy distribution fitting to determine GJ 581's effective surface temperature and its luminosity. From these measurements, they recomputed the location and extent of the system's habitable zone and conclude that two of the planets orbiting GJ 581 spend all or part of their orbit within or just on the edge of the habitable zone.

The bright star 55 Cancri is known to host five planets, including a transiting super-Earth. The study performed by von Braun et al. (2011b) yielded directly determined values for 55 Cnc's stellar astrophysical parameters based on improved interferometry at CHARA Array. Their analysis of the location and extent of the system's habitable zone (0.67–1.32 AU) shows that planet 55 Cnc f, with period ~ 260 days and $M \sin i = 0.155$ $M_{\rm Jupiter}$, spends the majority of the duration of its elliptical orbit in the circumstellar habitable zone. Though the planet is too massive to harbor liquid water on any planetary surface, they elaborate on the potential of alternative low-mass objects in planet's vicinity: a large moon, and a low-mass planet on a dynamically stable orbit within the habitable zone. Finally, their direct value for 55 Cancri's stellar radius allowed for a model-independent calculation of the physical diameter of the transiting super-Earth 55 Cnc e ($\sim 2.05 \pm 0.15$ $R_{\oplus}$), which, depending on the planetary mass assumed, implied a bulk density between 0.76 $\rho_{\oplus}$and $1.07\rho_{\oplus}$.

15. GALACTIC CENTER

With suffcient intensity sensitivity, the current large-aperture optical-long-baseline interferometers with baselines ~ 100 m provide the unique capability to study the Galactic Center (GC) sources. The massive black hole Sgr A* at the very center of our Galaxy, and its immediate stellar and non-stellar environment, have been studied in the past decade with increasing intensity and wavelength coverage. This research requires the highest angular resolution available to avoid source confusion and to study the physical properties and peculiarities of extreme individual objects in the central stellar cluster which contribute to our knowledge of star and dust formation close to the black hole.

The first VLTI detection of a star in the GC was achieved in 2004; the dust enshrouded star GCIRS 3 in the central light year of our galaxy was partially resolved in VLTI/MIDI N-band by Pott et al. (2005) GCIRS 3, is the prominent MIR-source in the central parsec of the Galaxy for which NIR spectroscopy has failed to solve the enigma of its nature. Pott et al. (2008a) initiated an interferometric experiment to understand the nature of GCIRS 3 where they investigate its properties as a spectroscopic and interferometric reference star at 10 μm using VLT/VISIR imaging (Fig. 20) which separated a compact source from diffuse, surrounding emission. The VLTI/MIDI instrument was used to measure

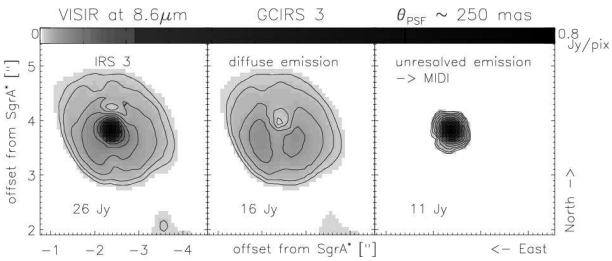

Fig. 20. *The diffuse emission from GCIRS 3. The VISIR 8.6 μm imaging data of a 4 arcsec field of view centered on GCIRS 3. Left: the diffuse emission as observed. Middle: the diffuse emission with subtracted PSF. Right: the flux-calibrated PSF, i.e. the unresolved emission seen by MIDI. All images have the same gray level coding as indicated at the top and the same contour lines for ease of comparison.*

spectroscopically resolved visibility moduli. The coinciding interpretation of single telescope and interferometric data confirmed dust emission from several different spatial scales; the interferometric data resolved the inner rim of dust formation. They concluded that the observed silicate absorption most probably takes place in the outer diffuse dust, which was mostly ignored by MIDI measurements, but very observable in complementary VLT/VISIR data. This indicated physically and chemically distinct conditions of the local dust, changing with the distance to GCIRS 3.

The next step was to study GCIRS 7 which is the dominating star of the central cluster in the NIR, so it has been used as wavefront and astrometric reference. In order to investigate, for the first time, its properties at 2 and 10 μm, Pott et al. (2008b) used VLTI-AMBER and MIDI instruments to spatially resolve the object and to measure the wavelength dependence of the visibility. The MIR data confirmed recent findings of a relatively enhanced, interstellar 9.8 μm-silicate absorption, suggesting an unusual dust composition in that region.

16. ACTIVE GALACTIC NUCLEI

Active galactic nuclei (AGNs) reside in centers of galaxies and emit radiation over the entire electromagnetic spectrum, from the most energetic gamma-ray photons up to the longest radio waves. Dusty tori have been suggested to play a crucial role in determining the physical characteristics of active galactic nuclei, but this explanation remained unproved, as even the largest telescopes have not been able to resolve the dust structures and investigation of tori properties has stalled for lack of high resolution mid-infrared imaging. A great step forward in the quality of interferometric data provided by large optical telescopes allowed recently to study interferometrically at least the brightest AGNs.

The most studied object in the past was the NGC 1068, the nearby AGN, which is an archetype type 2 Seyfert galaxy and bright enough to be observed even in pre-VLTI/KI era. Observations of this object corroborated with theoretical modeling like radiative transfer calculations have made signiffcant contributions on its structure. Ebstein et al. (1989) found a bipolar structure of this object in the [OIII] emission line. Near-IR observations at the Keck I telescope traced a very compact central core and extended emission with a size of the order of 10 pc on either side of an unresolved nucleus (Weinberger et al. 1999). Wittkowski et al. (1998) have resolved central 2.2 μm core by bispectrum speckle interferometry at the diffraction-limit of the Special Astrophysical Observatory 6m telescope with a FWHM size of $\sim$ 2 pc for an assumed Gaussian intensity distribution. Recently, breakthrough in the field was achieved: NGC 1068, was the first extragalactic object to be observed with a mid-IR interferometer, thereby obtaining the needed angular resolution to study the alleged torus.

Jaffe et al. (2004) reported interferometric mid-infrared observations that spatially resolve the central dusty torus in the active nucleus of the galaxy NGC 1068 (Fig. 21). The observations reveal warm (320K) dust in a structure 2.1 parsec thick and 3.4 parsec in diameter, surrounding a smaller hot structure. As such a configuration of dust clouds would collapse in a time much shorter than the active phase of the AGN, this model required a continual input of kinetic energy to the cloud system from a source coexistent with the AGN.

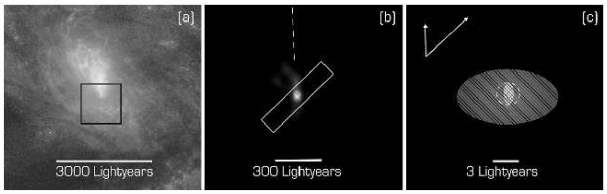

Fig. 21. *The core of the AGN galaxy NGC 1068. a) Optical image of the central region of NGC 1068 taken with the Hubble Space Telescope. The black square centred on the dust-obscured nucleus marks the region of b. b) Single-telescope acquisition image (deconvolved) of NGC 1068 taken by MIDI with a 8.7 μm filter penetrating the dust and showing the structures on arcsec scales. Also shown is the position of the spectroscopic slit used in the interferometric observations. c) Model dust structure in the nucleus of NGC 1068. It contains a central hot component (dust temperature T> 800 K) marginally resolved along the source axis.*

Wittkowski et al. (2004b) presented the first near-infrared K-band long-baseline interferometric measurement of the nucleus of the NGC 1068 with resolution $\sim$ 10 mas obtained with the VLTI/VINCI and the two 8.2 m diameter Unit Telescopes. Taking into account K-band speckle interferometry observations (Wittkowski et al. 1998, Weinberger et al. 1999, Weigelt et al. 2004), they favored a multi-component model for the intensity distribution where a part of the flux originates from scales smaller than $\sim$5 mas ($\approx$0.4 pc), and another part of the flux from larger scales. They argue that the K-band emission from the small ($\sim$5 mas) scales might arise from a substructure of the dusty nuclear torus, or directly from the central accretion flow viewed through only moderate extinction.

Poncelet et al. (2006) presented a new analysis of the first mid-infrared N-band long-baseline interferometric observations of an extragalactic source: the nucleus of the NGC 1068, obtained with the VLTI/MIDI instrument. The resolution of 10 mas allowed to study the compact central core of the galaxy between 8 and 13 μm. Both visibility measurements and MIDI spectrum were well reproduced by a radiative transfer model with two concentric spherical components. The derived angular sizes and temperatures are $\sim$ 35 and 83 mas, and $\sim$ 361 K and 226 K for these two components respectively. This modeling also provided the variation of the optical depth as a function of wavelength for the extended component across the N-band suggesting the presence of

amorphous silicate grains. Poncelet et al. (2007) presented 12.8 μm images of the core of NGC 1068, obtained with the VLT/VISIR (Imager and Spectrometer in the InfraRed). A speckle processing of raw images was performed to extract very low spatial-frequency visibilities, first considering the full field images and then limiting it to the mask used for the acquisition of MIDI data. Extracted visibilities were reproduced with a multi-component model. They identify two major sources of emission at 12.8 μm: a compact one <85 mas, directly associated with the dusty torus, and an elliptical one of size (<140) mas $\times$ 1187 mas and PA $\sim -4°$(from north to east).

In order to resolve the obscuring torus in NGC 1068, Raban et al. (2009) obtained interferometric data with the VLTI/MIDI, with an extensive u, v coverage. These observations resolved the nuclear mid-infrared emission from NGC 1068 in unprecedented detail with a maximum resolution of 7 mas, allowing to generate an image of the source using the maximum entropy image reconstruction (Fig. 22). The mid-infrared emission could be represented by two components: The first, identified as the inner funnel of the obscuring torus, is hot ($\sim$800K), 1.35 parsec long and 0.45 parsec thick with evidence for clumpiness. The compact component is tilted by $\sim 45°$with respect to the radio jet and has similar size and orientation to the observed water maser distribution. The second component is 3 pc $\times$ 4 pc with $T =\sim$ 300K, is identified as the cooler body of the torus. They showed how the dust distribution relates to other observables within a few parsec of the core of the galaxy, such as the nuclear masers, the radio jet and the ionization cone (Fig. 23).

Centaurus A close distance of only 3.84 Mpc offers unique opportunities to look into the very core

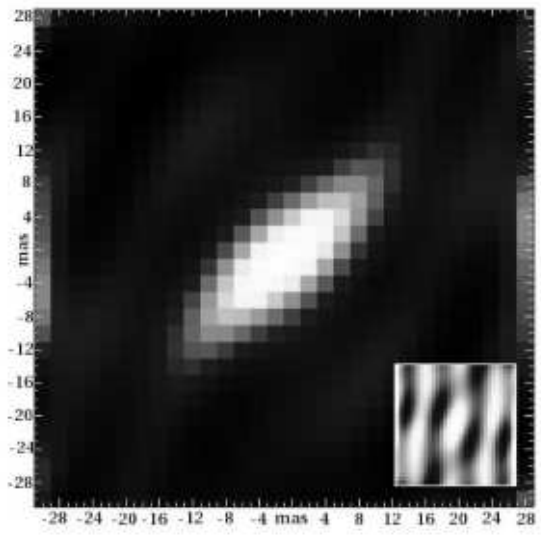

Fig. 22. *Maximum entropy reconstruction of NGC 1068 at 8 μm. Image size is 30 $\times$ 30 pixels, with 1 pix = 2 mas. The "dirty map" (point spread function) is shown in the bottom left corner.*

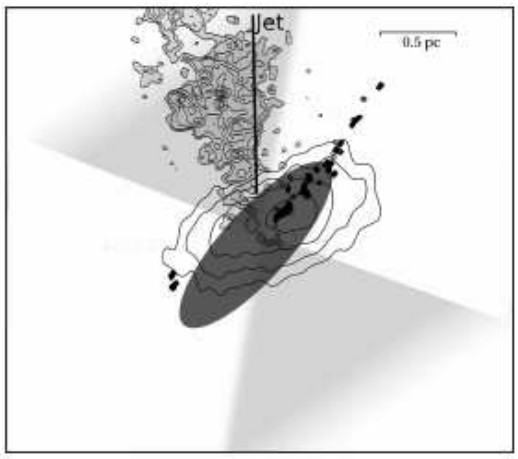

Fig. 23. *Multi-wavelength structures on parsec-scales in the nucleus of NGC 1068. The fit of the compact dust is sketched in dark gray, centred around the H_2O maser spots and 5 GHz radio emission. The ionization cones inferred from spectroscopy and the HST [OIII] image contours are shown as well.*

of an AGN, as 1 parsec corresponds to 53 mas. Despite this fact, single-telescope observations have not been able to resolve the core at any wavelength while radio interferometry with VLBI networks revealed a core - jet structure within the central parsec: the well-collimated radio jet could be traced over > 60 mas atλ = 6cm. In order to complement radio interferometry and to reveal the origin of mid-infrared radiation from the core of Centaurus A, Meisenheimer et al. (2007) carried out interferometric observations with the VLTI/MIDI. Observations were obtained with four baselines between unit telescopes of the VLTI, two of them roughly along the radio axis and two orthogonal to it. The interferometric measurements were spectrally resolved with R=30 in the wavelength range 8 to 13 μm, reaching 15 mas resolution at the shortest wavelengths. Considering the mid-infrared emission from the core of Centaurus A which is dominated by an unresolved point source (<10 mas), they estimate a thermal luminosity of the core to be intermediate between the values for highly efficiently accreting AGN and those of typical radio galaxies, concluding that this luminosity, which is predominantly released in X-rays, is most likely generated in an advection dominated accretion flow. Burtscher et al. (2010) have observed Centaurus A with the VLTI/MIDI at resolutions of 7-15 mas (at 12.5 μm) and filled gaps in the (u, v) coverage in comparison to earlier measurements. They were able to describe the nuclear emission in terms of geometric components and derive their parameters by fitting models to the interferometric data.

To test the dust torus model for active galactic nuclei directly, Tristram et al. (2007) studied the extent and morphology of the nuclear dust distribution in the Circinus galaxy using high resolution interferometric observations in the mid-infrared at VLTI/MIDI instrument. They find that the dust

distribution in the nucleus can be explained by two components, a dense and warm disc-like component of 0.4 pc size and a slightly cooler, geometrically thick torus component with a size of 2.0 pc. The disc component is oriented perpendicular to the ionisation cone and outflow, and seems to show the silicate feature at 10 μm in emission, coinciding with a nuclear maser disc in orientation and size. From the energy needed to heat the dust, they infer a luminosity of the accretion disc of $L_{\rm acc}$= 10^{10} $L_{\odot}$, which corresponds to 20 % of the Eddington luminosity of the nuclear black hole. They find that the interferometric data are inconsistent with a simple, smooth and axisymmetric dust emission; the irregular behaviour of the visibilities and the shallow decrease of the dust temperature with radius provide strong evidence for a clumpy or filamentary dust structure and they argue that the collimation of the ionising radiation must originate in the geometrically thick torus component.

Beckert et al. (2008) presented the mid-IR spectro-interferometry of the Seyfert type 1 nucleus of NGC 3783. In order to spatially resolve the dusty circumnuclear environment and deduce the wavelength dependence of the compact emission, the observations were carried out with the VLTI/MIDI instrument in the N-band. They find that the mid-IR emission from the nucleus can be reproduced by an extended dust disc or torus with a small covering factor of the radiating dust clouds which supported a clumpy version of the unified scheme for AGN. Tristram et al. (2009) carried out in a "snapshot survey" with VLTI/MIDI attempting observations for 13 of the brightest AGN in the mid-infrared. Their results indicate that the dust distributions are compact, with sizes on the order of a few parsec, and they conclude that in the mid-infrared the differences between individual galactic nuclei are greater than the generic differences between the type 1 and type 2 objects.

Swain et al. (2003) have observed the nucleus of NGC 4151 at 2.2 μm using the two 10 m Keck telescopes and find a marginally resolved source $\leq$ 0.1 pc in diameter, ruling out models in which a majority of the K-band nuclear emission is produced on scales larger than this size. The interpretation of their measurement most consistent with other observations is that the emission mainly originates directly in the central accretion disc, which implied that active galactic nucleus unification models invoking hot, optically thick dust may not be applicable to NGC 4151. Kishimoto et al. (2009) reported successful observations with the Keck interferometer at K-band (2.2 μm) for four type 1 AGNs, namely NGC 4151, Mrk231, NGC 4051, and the QSO IRAS 13349+2438, for the latter three objects, these were the first long-baseline interferometric measurements in the infrared. They detected high visibilities (V^2 $\sim$ 0.8-0.9) for all the four objects including NGC 4151, for which they confirmed the high visibility level measured by Swain et al. (2003).

Burtscher et al. (2009) reported mid-infrared interferometric measurements with $\sim$ 10 mas resolution, which resolved the warm ($T \sim 290$ K) thermal emission at the center of NGC 4151, using pairs of UT 8.2 m telescopes with the VLTI/MIDI instrument. They determined the diameter of the dust emission region, providing the first size and temperature estimate for the nuclear warm dust distribution in a Seyfert 1 galaxy. The deduced parameters are comparable to those in Seyfert 2 galaxies, thus providing direct support for the unified model (contrary to the conclusion of Swain et al. (2003)). Using simple analytic temperature distributions, they find that the mid-infrared emission is probably not the smooth continuation of the hot nuclear source that was marginally resolved with K-band interferometry. They also detected weak excess emission around 10.5 μm in shorter baseline observation, indicating that silicate emission is extended to the parsec scale. After recent sensitivity upgrades at the Keck Interferometer (KI), an interferometric 2 μm study of the innermost dust in nearby Seyfert nuclei was performed by Pott et al. (2010) who presented the analysis of new interferometric data of NGC 4151. Their data set gives a complex picture, in particular the measured visibilities from three different nights appear to be rather insensitive to the variation of the nuclear luminosity while the interferometric, deprojected centro-nuclear dust radius estimate of 55 $\pm$ 5 mpc is roughly consistent with the earlier published expectations from circum-nuclear, dusty radiative transfer models, and spectro-photometric modeling.

Kishimoto et al. (accepted 2011) presented mid-IR interferometric VLTI/MIDI observations of six type 1 AGNs: NGC 4151, NGC 3783, ESO323-G77, H0557-385, IRAS09149 and IRAS13349, at multiple baselines up to 130m reaching high angular resolutions up to 0.02 arc-seconds. They found that all the objects were partially resolved at long baselines, thus directly probing the radial distribution of the AGN tori material on sub-pc scales.

17. IMAGE RECONSTRUCTION

Since the interferometers do not directly provide images, reconstruction methods are needed to fully exploit these instruments. As it was shown in this review there are numerous astrophysical applications of image reconstruction and the field of possible applications is permanently growing. Particularly taking into account that the enhanced auxiliary telescope array at the VLTI and the proposed outrigger telescopes at Keck will allow fainter targets to be observed. Even the existing configurations, complemented with aperture masking at large single telescopes and other interferometeric arrays allow a number of yet unexplored objects to be studied. In addition to previously mentioned image reconstructions, here I list some recent outstanding results proving this trend: Monnier et al. (2004) presented first results of an experiment to combine data from Keck aperture masking and the Infrared Optical Telescope Array (IOTA) to image the circumstellar environments of evolved stars with $\sim$ 20 mas resolution. The unique combination of excellent Fourier coverage at short baselines and high-quality

long-baseline data allowed them to determine the location and clumpiness of the innermost hot dust in the envelopes and to measure the diameters of the underlying stars themselves. They find evidence for large-scale inhomogeneities in some dust shells and also significant deviations from uniform brightness for the photospheres of the most evolved M stars.

Kraus et al. (2005) presented infrared aperture synthesis maps of close binary system Capella (α Aur) produced with the upgraded IOTA interferometer using the IONIC3 beam recombiner. With baselines of 15 m $\leq B \leq$ 38 m, they were able to determine the relative position of the binary components with milli-arcsecond precision. The resulting model-independent map with a beam size of 5.4 mas $\times$ 2.6 mas allows the resolution of the stellar surfaces of the Capella giants themselves. Using the optical long-baseline interferometry at CHARA, Monnier et al. (2007) reconstructed a near-infrared image of the rapidly rotating hot star Altair (Fig. 24) with a resolution of < 1 mas. The image clearly reveals the strong effect of gravity darkening on the highly distorted stellar photosphere. Standard models for a uniformly rotating star could not explain their findings, which appear to result from differential rotation, alternative gravity-darkening laws, or both.

First resolved images of the eclipsing and interacting binary β Lyrae have been reported by Zhao et al. (2008) using observations with the CHARA/MIRC recombiner in the H band. The images (Fig. 25) clearly show the mass donor and the thick disc surrounding, the mass gainer, at all six epochs of observation. The donor is brighter and generally appears elongated in the images, the first direct detection of photospheric tidal distortion due to Roche lobe filling. They also confirm expectations that the disc component is more elongated than the donor and is relatively fainter at this wavelength.

Schmitt et al. (2009) presented the results of imaging the interacting binary star β Lyrae with data from the Navy Prototype Optical Interferometer (NPOI) using a differential phase technique.

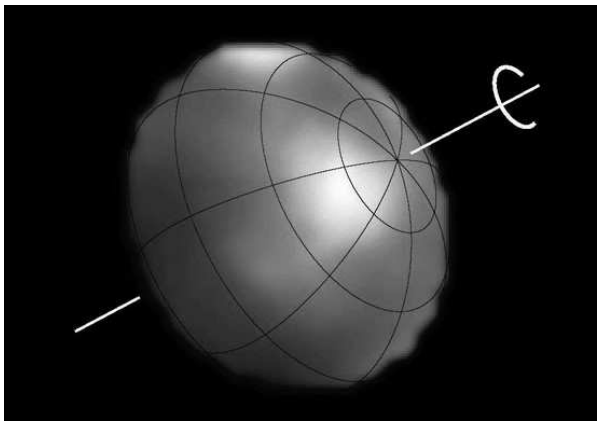

Fig. 24. *Reconstructed image of Altair. Image of Altair from the CHARA interferometer which clearly reveals the strong effect of gravity darkening on the highly distorted stellar photosphere.*

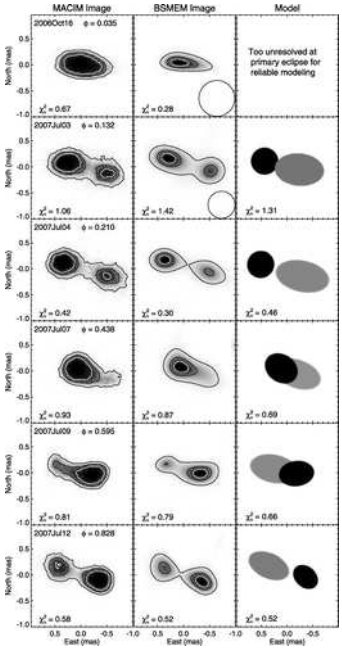

Fig. 25. *Reconstructed images and two-component models of β Lyr. The left, middle, and right columns show two different image reconstructions (Zhao et al. 2008), and model images, respectively and darker indicate higher intensity. The darker component is the donor.*

Combining the Hα-channel phases with information about the line strength, they recovered complex visibilities and imaged the Hα emission using standard radio interferometry methods. Their images show the position of the Hα-emitting regions relative to the continuum photocenter as a function of orbital phase.

The first images of the symbiotic long-period Mira variable R Aqr and its asymmetric H_2O shell have been reported by Ragland et al. (2008) using observations at near-infrared and radio wavelengths. The near-infrared observations were made with the IOTA imaging interferometer in three narrowband filters centered at 1.51, 1.64, and 1.78 μm, which sample mainly water, continuum, and water features, respectively. A model generated by a constrained image reconstruction analysis provides more insight, suggesting that the water shell is highly nonuniform, i.e. clumpy. Thureau et al. (2009) presented the first high angular resolution observation of the B[e] star/X-ray transient object CI Cam, performed with the two-telescope IOTA, its upgraded three-telescope version (IOTA 3T) and the Palomar Testbed Interferometer (PTI). The star was observed in the near-infrared H and K spectral bands, wavelengths well suited to measure the size and study the geometry of the surrounding hot dust. The visibility data showed that CI Cam is elongated which confirms the disc-shape of the circumstellar environment and totally rules out the hypothesis of a spherical dust shell, while closure phase measurements show

a direct evidence of asymmetries in the circumstellar environment, leading to the conclusion that the dust surrounding CI Cam lies in an inhomogeneous inclined disc.

Millour et al. (2009b) observed HD 87643 with high spatial resolution techniques, using the near-IR VLTI/AMBER and the mid-IR VLTI/MIDI interferometer, complemented by NACO/VLT adaptive-optics-corrected images in the K and L-bands, as well as ESO-2.2 m optical Wide-Field Imager images in the B, V and R-bands. They reported the direct detection of a companion to HD 87643 by means of image synthesis concluding that the binarity with high eccentricity might be the key to interpreting the extreme characteristics of this system, namely a dusty circumstellar envelope around the primary, a compact dust nebulosity around the binary system and a complex extended nebula suggesting past violent ejections.

In order to explore the photosphere of the very cool late-type star VX Sgr and in particular the characterization of molecular layers above the continuum forming photosphere. Chiavassa et al. (2010) obtained interferometric observations with the VLTI/AMBER instrument. Reconstructed images and visibilities showed a strong wavelength dependence, and the H-band images display two bright spots whose positions are confirmed by the geometrical model. At ≈ 2.00 μm and in the region 2.35-2.50 μm, the geometrical model locates a third bright spot outside the photosphere that can be a feature of the molecular layers, the H_2O being the dominant absorber in the molecular layers.

With the purpose of testing various mass-ejection processes, Millour et al. (2011) probed the geometry and kinematics of the dust and gas surrounding the A[e] supergiant HD 62623, using the combined high spectral and spatial resolution provided by the VLTI/AMBER instrument. Using a multiwavelength optical/IR interferometry imaging technique as presented in Fig. 26, they reconstructed the first velocity-resolved images with a milli-arcsecond resolution in the infrared domain (Fig. 27). They managed to disentangle the dust and gas emission in the HD 62623 circumstellar disc, measured the inner gaseous disc extension and probed its velocity field, finding that the expansion velocity is negligible, and that Keplerian rotation is a dominant velocity field.

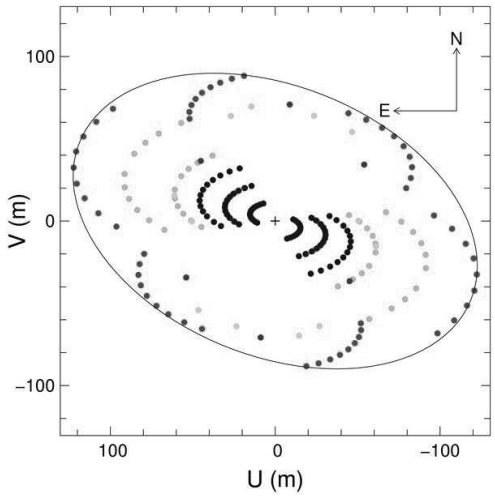

Fig. 26. *The u, v coverage of HD 62623 observations. Different gray levels represent different nights. The ellipse has dimensions* 82×128 *m.*

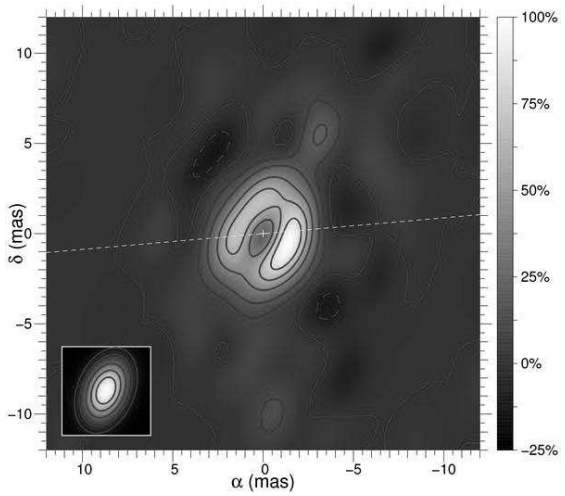

Fig. 27. *Line-integrated flux from HD62623. The PSF function is depicted at bottom left.*

18. CONCLUSION

Traditionally, optical interferometry has been considered as a tool to determine the fundamental properties of stars, namely their effective temperatures, radii, luminosities and masses, by the combination of angular diameters with complementary photometric, and spectroscopic measurements, made with conventional telescopes. However, the impact of interferometry on stellar physics extended beyond classical applications and now, based on a great leap forward in the quality and quantity of interferometric data, the field is currently driven forward by the activities in many research areas. Thus, important scientific results have been obtained, particularly in the past decade.

Major interferometers such as VLTI and KI have started science operation and have boosted the rate of astrophysics-oriented publications based on interferometric results. Also, the advent of long-baseline interferometers making use of large pupils has opened the way to faint science and first results on extragalactic objects has made it a reality.

The first decade of the 21st century is also remarkable for aperture synthesis in the visual and near-infrared wavelength regimes which provided image reconstructions from stellar surfaces to Active Galactic Nuclei. The range of application is rapidly growing, as well as the support from the image reconstruction community, and, in the near future, the technique will be applied in the manner that instead of being an exciting experiment it will become a routine operation.

Acknowledgements – This work has been supported by the Ministry of Education and Science of the Republic of Serbia (Project No. 176004 "Stellar physics").

REFERENCES

Absil, O., di Folco, E., Mérand, A., Augereau, J.-C., Coudé Du Foresto, V., et al.: 2006, *Astron. Astrophys.*, **452**, 237.
Absil, O., di Folco, E., Mérand, A., Augereau, J.-C., Coudé Du Foresto, V., et al.: 2008, *Astron. Astrophys.*, **487**, 1041.
Akeson, R. L., Ciardi, D. R., van Belle, G. T., Creech-Eakman, M. J., and Lada, E. A.: 2000, *Astrophys. J.*, **543**, 313.
Akeson, R. L., Ciardi, D. R., van Belle, G. T., and Creech-Eakman, M. J. 2002, *Astrophys. J.*, **566**, 1124.
Akeson, R. L., Walker, C. H., Wood, K., Eisner, J. A., Scire, E., et al.: 2005a, *Astrophys. J.*, **622**, 440.
Akeson, R. L., Boden, A. F., Monnier, J. D., Millan-Gabet, R., Beichman, C., et al.: 2005b, *Astrophys. J.*, **635**, 1173.
Armstrong, J. T., Nordgren, Tyler E., Germain, M. E., Hajian, et al.: 2001, *Astron. J.*, **121**, 476.
Armstrong, J. T., Mozurkewich, D., Hajian, Arsen R., Johnston, K. J., et al.: 2006, *Astron. J.*, **131**, 2643A.
Aufdenberg, J. P., Mérand, A., Coudé du Foresto, V., Absil, O., Di Folco, E. et al.: 2006a, *Astrophys. J.*, **645**, 664.
Aufdenberg, J. P., Mérand, A., Coudé du Foresto, V., Absil, O., Di Folco, E., et al.: 2006b, *Astrophys. J.*, **651**, 617.
Baines, E. K., van Belle, G. T., ten Brummelaar, T. A., McAlister, H. A., Swain, M., et al.: 2007, *Astrophys. J.*, **661**, L195.
Baines, E. K., McAlister, H. A., ten Brummelaar, T. A., Turner, N. H., Sturmann, J., et al.: 2008, *Astrophys. J.*, **680**, 728.
Baines, E. K., McAlister, H. A., ten Brummelaar, T. A., Sturmann, J., Sturmann, L., et al.: 2009, *Astrophys. J.*, **701**, 154.
Baines, E. K., McAlister, H. A., ten Brummelaar, T. A., Turner, N. H., Sturmann, J. et al.: 2010, *Astron. J.*, **140**, 167.
Baldwin J. E., Haniff C. A., Mackay C. D. and Warner P. J.,: 1986, *Nature*, **320**, 595.
Barry, R. K., Danchi, W. C., Traub, W. A., Sokoloski, J. L., Wisniewski, J. P., et al.: 2008, *Astrophys. J.*, **677**, 1253.
Beckers, J. M.: 1982, *Optica Acta*, **29**, 361.
Beckert, T., Driebe, T., Hönig, S. F., Weigelt, G.: 2008, *Astron. Astrophys.*, **486**, L17.
Beckwith, S. V. W., Sargent, A. I., Chini, R. S., and Guesten, R.: 1990, *Astron. J.*, **99**, 924.
Benisty, M., Natta, A., Isella, A., Berger, J.-P., Massi, F., et al.: 2010, *Astron. Astrophys.*, **511**, 74.
Bigot, L., Kervella, P., Thévenin, F., Ségransan, D.: 2006, *Astron. Astrophys.*, **446**, 635.
Bigot, L., Mourard, D., Berio, P., Thévenin, F., Ligi, R., et al.: 2011, *Astron. Astrophys.*, **534**, L3.
Boboltz, D. A., Wittkowski, M.: 2005, *Astrophys. J.*, **618**, 953.
Bonneau D., and Foy R.: 1980, *Astron. Astrophys.*, **92**, L1.
Boyajian, T. S., McAlister, H. A., Cantrell, J. R., Gies, D. R., ten Brummelaar, T. A., et al.: 2009, *Astrophys. J.*, **691**, 1243.
Bruntt, H., North, J. R., Cunha, M., Brandão, I. M., Elkin, V. G., et al.: 2008, *Mon. Not. R. Astron. Soc.*, **386**, 2039.
Bruntt H., Kervella P., Mérand A., Brandão I. M., Bedding, T. R. et al.: 2010, *Astron. Astrophys.*, **512**, 55.
Bujarrabal, V., van Winckel, H., Neri, R., Alcolea, J., Castro-Carrizo, A., Deroo, P.: 2007, *Astron. Astrophys.*, **468**, L45.
Burns, D., Baldwin, J. E., Boysen, R. C., Haniff, C. A., Lawson, P. R. et al.: 1997, *Mon. Not. R. Astron. Soc*, **290**, L11.
Burtscher, L., Jaffe, W., Raban, D., Meisenheimer, K., Tristram, K. R. W., Röttgering, H., 2009, *Astrophys. J.*, **705**, L53.
Burtscher, L., Meisenheimer, K., Jaffe, W., Tristram, K. R. W., Röttgering, H. J. A.: 2010, *Publ. Astron. Soc. Australia*, **27**, 490.
Buscher D. F., Baldwin J. E., Warner P. J. and Haniff C. A.: 1990, *Mon. Not. R. Astron. Soc.*, **245**, 7.
Carciofi, A. C., Domiciano de Souza, A., Magalhães, A. M., Bjorkman, J. E., Vakili, F.: 2008, *Astrophys. J.*, **676**, L41.
Chandler, A. A., Tatebe, K., Wishnow, E. H., Hale, D. D. S., Townes, C. H.: 2007, *Astrophys. J.*, **670**, 1347.
Chesneau, O., Meilland, A., Rivinius, T., Stee, Ph., Jankov, S., et al.: 2005a, *Astron. Astrophys.*, **435**, 275.
Chesneau, O., Min, M., Herbst, T., Waters, L. B. F. M., Hillier, D. J., et al.: 2005b, *Astron. Astrophys.*, **435**, 1043.
Chesneau, O., Collioud, A., De Marco, O., Wolf, S., Lagadec, E., et al.: 2006, *Astron. Astrophys.*, **455**, 1009.
Chesneau, O., Lykou, F., Balick, B., Lagadec, E., Matsuura, M., et al.: 2007a, *Astron. Astrophys.*, **473**, L29.
Chesneau, O., Nardetto, N., Millour, F., Hummel, C., Domiciano de Souza, A., et al.: 2007b, *Astron. Astrophys.*, **464**, 119.
Chesneau, O., Banerjee, D. P. K., Millour, F., Nardetto, N., Sacuto, S., et al.: 2008, *Astron. Astrophys.*, **487**, 223.
Chesneau, O., Meilland, A., Banerjee, D. P. K., Le Bouquin, J.-B., McAlister, H., et al.: 2011, *Astron. Astrophys.*, **534**, L11.
Chiavassa, A., Lacour, S., Millour, F., Driebe, T., Wittkowski, M., et al.: 2010, *Astron. Astrophys.*, **511**, 51.
Churchwell, E., Wolfire, M., and Wood, D.: 1990, *Astrophys. J.*, **354**, 247.
Colavita, M., Akeson, R., Wizinowich, P., Shao, M., Acton, S., et al.: 2003, *Astrophys. J.*, **592**, L83.
Danchi, W. C., Tuthill, P. G., Monnier, J. D.: 2001, *Astrophys. J.*, **562**, 440.
Davis, J.: 1976, *Proc. Astron. Soc. Australia*, **3**, 26.

Davis, J., Jacob, A. P., Robertson, J. G., Ireland, M. J., North, J. R., et al.: 2009, *Mon. Not. R. Astron. Soc.*, **394**, 1620.
Delbo, M., Ligori, S., Matter, A., Cellino, A., Berthier, J.: 2009, *Astrophys. J.*, **694**, 1228.
Demory, B.-O., Ségransan, D., Forveille, T., Queloz, D., Beuzit, J.-L., et al.: 2009, *Astron. Astrophys.*, **505**, 205.
Denker, C.: 1998, *Solar Phys.*, **81**, 108.
Deroo, P., van Winckel, H., Min, M., Waters, L. B. F. M., Verhoelst, T., et al.: 2006, *Astron. Astrophys.*, **450**, 181.
de Wit, W. J., Hoare, M. G., Oudmaijer, R. D., Mottram, J. C.: 2007, *Astrophys. J.*, **671**, L169.
de Wit, W. J., Hoare, M. G., Oudmaijer, R. D., Lumsden, S. L.: 2010, *Astron. Astrophys.*, **515**, 45.
di Folco, E., Absil, O., Augereau, J.-C., Mérand, A., Coudé Du Foresto, V., et al.: 2007, *Astron. Astrophys.*, **475**, 243.
di Folco, E., Dutrey, A., Chesneau, O., Wolf, S., Schegerer, A., et al.: 2009, *Astron. Astrophys.*, **500**, 1065.
Domiciano de Souza, A., Vakili, F., Jankov, S., Janot-Pacheco, E., Abe, L.: 2002, *Astron. Astrophys.*, **393**, 345.
Domiciano de Souza, A., Kervella, P., Jankov, S., Abe, L., Vakili, F., et al.: 2003, *Astron. Astrophys.*, **407**, L47.
Domiciano de Souza, A., Kervella, P., Jankov, S., Vakili, F., Ohishi, N., et al.: 2005, *Astron. Astrophys.*, **442**, 567.
Domiciano de Souza, A., Driebe, T., Chesneau, O., Hofmann, K.-H., Kraus, S., et al.: 2007, *Astron. Astrophys.*, **464**, 81.
Drummond J., Eckart, A. and Hege E.: 1988, *Icarus*, **73**, 1.
Dullemond, C. P.; Dominik, C.; Natta, A.: 2001, *Astrophys. J.*, **560**, 957.
Ebstein S., N. P. Carleton, and C. Papaliolios, 1989, *Astrophys. J.*, **336**, 103.
Eisner, J. A., Lane, B. F., Akeson, R. L., Hillenbrand, L. A., Sargent, A. I.: 2003, *Astrophys. J.*, **588**, 3.
Eisner, J. A., Lane, B. F., Hillenbrand, L. A., Akeson, R. L., Sargent, A. I.: 2004, *Astrophys. J.*, **613**, 1049.
Eisner, J. A., Hillenbrand, L. A., White, R. J., Akeson, R. L., Sargent, A. I.: 2005, *Astrophys. J.*, **623**, 952.
Eisner, J. A., Chiang, E. I., Lane, B. F., Akeson, R. L.: 2007b, *Astrophys. J.*, **657**, 347.
Eisner, J. A., Graham, J. R., Akeson, R. L., Ligon, E. R., Colavita, M. M., et al.: 2007a, *Astrophys. J.*, **654**, L77.
Eisner, J. A., Hillenbrand, L. A., White, R. J., Bloom, J. S., Akeson, R. L., Blake, C. H.: 2007c, *Astrophys. J.*, **669**, 1072.
Eisner, J. A., Graham, J. R., Akeson, R. L., Najita, J.: 2009, *Astrophys. J.*, **692**, 309.
Fedele, D., Wittkowski, M., Paresce, F., Scholz, M., Wood, P. R., Ciroi, S.: 2005, *Astron. Astrophys.*, **431**, 1019.
Follert, R., Linz, H., Stecklum, B., van Boekel, R., Henning, Th., et al.: 2010, *Astron. Astrophys.*, **522**, 17.
Gies, D. R., Bagnuolo, W. G., Jr., Baines, E. K., ten Brummelaar, T. A., Farrington, C. D., et al.: 2007, *Astrophys. J.*, **654**, 527G.
Groh, J. H., Madura, T. I., Owocki, S. P., Hillier, D. J., Weigelt, G.: 2010, *Astrophys. J.*, **716**, L223.
Haniff C. A., Mackay C. D., Titterington D. J., Sivia D. and Baldwin J. E.: 1987, *Nature*, **328**, 694.
Harvey J. W.: 1972, *Nature*, **235**, 90.
Harvey J. W., and Breckinridge J. B.: 1973, *Astrophys. J.*, **182**, L137.
Haubois, X., Perrin, G., Lacour, S., Verhoelst, T., Meimon, S., et al.: 2009, *Astron. Astrophys.*, **508**, 923.
Hofmann, K.-H., Beckmann, U., Blöcker, T., Coudé du Foresto, V., Lacasse, M., et al.: 2002, *New Astron.*, **7**, 9.
Ireland, M. J., Tuthill, P. G., Davis, J., Tango, W.: 2005, *Mon. Not. R. Astron. Soc.*, **361**, 337.
Isella, A., Tatulli, E., Natta, A., Testi, L.: 2008, *Astron. Astrophys.*, **483**, L13.
Jackson, S., MacGregor, K. B., Skumanich, A.: 2004, *Astrophys. J.*, **606**, 1196.
Jaffe, W., Meisenheimer, K., Röttgering, H. J. A., Leinert, Ch., Richichi, A., et al.: 2004, *Nature*, **429**, 47.
Jankov, S., Vakili, F., Domiciano de Souza, A., Jr., Janot-Pacheco, E.: 2001, *Astron. Astrophys.*, **377**, 721.
Jankov, S., Vakili, F., Domiciano de Souza Jr., A., Janot-Pacheco, E.: 2002, ASPCS, 259, eds.C. Aerts, T.R. Bedding and J. Christensen-Dalsgaard, 172.
Jankov, S., Vakili, F., Domiciano de Souza, A.: 2003a, Proceedings IAUS, **210**, D16.
Jankov, S., Domiciano de Souza, A., Stehle, C., Vakili, F., Perraut-Rousselet, K., Chesneau, O.: 2003b, Interferometry for Optical Astronomy II, SPIE, **4838**, 587.
Kalas, P., Graham, J. R., Chiang, E., Fitzgerald, M. P., Clampin, M. et al. 2008, *Science*, **322**, 1345.
Kervella, P., Coudé du Foresto, V., Perrin, G., Schöller, M., Traub, W. A., Lacasse, M. G.: 2001, *Astron. Astrophys.*, **367**, 876.
Kervella, P., Thévenin, F., Ségransan, D., Berthomieu, G., Lopez, B., et al.: 2003a, *Astron. Astrophys.*, **404**, 1087.
Kervella, P., Thévenin, F., Morel, P., Bordé, P., Di Folco, E.: 2003b, *Astron. Astrophys.*, **408**, 681.
Kervella, P., Thévenin, F., Morel, P., Berthomieu, G., Bordé, P., Provost, J.: 2004a, *Astron. Astrophys.*, **413**, 251.
Kervella, P., Nardetto, N., Bersier, D., Mourard, D., Coudé du Foresto, V.: 2004b, *Astron. Astrophys.*, **416**, 941.
Kervella, P., Bersier, D., Mourard, D., Nardetto, N., Fouqué, P., Coudé du Foresto, V.: 2004c, *Astron. Astrophys.*, **428**, 587.
Kervella, P., Fouqué, P., Storm, J., Gieren, W. P., Bersier, D., et al.: 2004d, *Astrophys. J.*, **604**, L113.
Kervella, P. and Domiciano de Souza, A.: 2006a, *Astron. Astrophys.*, **453**, 1059.
Kervella, P., Mérand, A., Perrin, G., Coudé Du Foresto, V.: 2006b, *Astron. Astrophys.*, **448**, 623.

Kervella, P.: 2007, *Astron. Astrophys.*, **464**, 1045.
Kervella, P., Fouqué, P.: 2008, *Astron. Astrophys.*, **491**, 855.
Kervella, P., Domiciano de Souza, A., Kanaan, S., Meilland, A., Spang, A., Stee, Ph.: 2009, *Astron. Astrophys.*, **493**, L53.
Kishimoto, M., Hönig, S. F., Antonucci, R., Kotani, T., Barvainis, R., et al.: 2009, *Astron. Astrophys.*, **507**, L57.
Kishimoto, M., Hönig, S. F., Antonucci, R., Millour, F., Tristram, K. R. W., Weigelt, G: 2011, *Astron. Astrophys.*, accepted.
Kraemer, K. E., Jackson, J. M., Deutsch, L. K., Kassis, M., Hora, J. L., et al.: 2001, *Astrophys. J.*, **561**, 282.
Kraus, S., Schloerb, F. P., Traub, W. A., Carleton, N. P., Lacasse, M., et al.: 2005, *Astron. J.*, **130**, 246K.
Kraus, S., Hofmann, K.-H., Benisty, M., Berger, J.-P., Chesneau, O., et al.: 2008a, *Astron. Astrophys.*, **489**, 1157.
Kraus, S., Preibisch, T. and Ohnaka, K.: 2008b, *Astrophys. J.*, **676**, 490.
Kraus, S., Hofmann, K.-H., Malbet, F., Meilland, A., Natta, A., et al.: 2009, *Astron. Astrophys.*, **508**, 787.
Kraus, S., Hofmann, K.-H., Menten, K. M., Schertl, D., Weigelt, G., et al.: 2010, *Nature*, **466**, 339.
Lacour, S., Meimon, S., Thiébaut, E., Perrin, G., Verhoelst, T., et al.: 2008, *Astron. Astrophys.*, **485**, 561.
Lacour, S., Thiébaut, E., Perrin, G., Meimon, S., Haubois, X., et al.: 2009, *Astrophys. J.*, **707**, 632.
Lagadec, E., Chesneau, O., Matsuura, M., De Marco, O., de Freitas Pacheco, J. A., et al.: 2006, *Astron. Astrophys.*, **448**, 203.
Lane, B. F., Kuchner, M. J., Boden, A. F., Creech-Eakman, M., Kulkarni, S. R.: 2000, *Nature*, **407**, 485.
Lane, B. F., Creech-Eakman, M. J., Nordgren, T. E.: 2002, *Astrophys. J.*, **573**, 330.
Lane, B. F., Retter, A., Eisner, J. A., Muterspaugh, M. W., Thompson, R. R., Sokoloski, J. L.: 2007, *Astrophys. J.*, **669**, 1150.
Lane, B. F., Sokoloski, J. L., Barry, R. K., Traub, W. A., Retter, A., et al.: 2007, *Astrophys. J.*, **658**, 520.
Le Bouquin, J.-B., Lacour, S., Renard, S., Thiébaut, E., Merand, A., Verhoelst, T.: 2009a, *Astron. Astrophys.*, **496**, L1.
Le Bouquin, J.-B., Absil, O., Benisty, M., Massi, F., Mérand, A., Stefl, S.: 2009b, *Astron. Astrophys.*, **498**, L41.
Leinert, Ch., van Boekel, R., Waters, L. B. F. M., Chesneau, O., Malbet, F., et al.: 2004, *Astron. Astrophys.*, **423**, 537.
Linz, H., Henning, Th., Feldt, M., Pascucci, I., van Boekel, R., et al.: 2009, *Astron. Astrophys.*, **505**, 655.
Malbet, F., and Bertout, C.: 1991, *Astrophys. J.*, **383**, 814.
Malbet, F., Berger, J.-P., Colavita, M. M., Koresko, C. D., Beichman, C., et al.: 1998, *Astrophys. J.*, **507**, L149.
Malbet, F., Lachaume, R., Berger, J.-P., Colavita, M. M., di Folco, E., et al.: 2005, *Astron. Astrophys.*, **437**, 627.
Malbet, F., Benisty, M., de Wit, W.-J., Kraus, S., Meilland, A., et al.: 2007, *Astron. Astrophys.*, **464**, 43.
Martić M., Lebrun, J.-C., Appourchaux, T., Korzennik, S. G.: 2004, *Astron. Astrophys.*, **418**, 295.
Matter, A., Vannier, M., Morel, S., Lopez, B., Jaffe, W., et al.: 2010, *Astron. Astrophys.*, **515**, 69.
Mazumdar, A., Mérand, A., Demarque, P., Kervella, P., Barban, C., et al.: 2009, *Astron. Astrophys.*, **503**, 521.
McAlister, H. A., ten Brummelaar, T. A., Gies, D. R., Huang, W., Bagnuolo, W. G., Jr., et al.: 2005, *Astrophys. J.*, **628**, 439.
Meilland, A., Stee, P., Vannier, M., Millour, F., Domiciano de Souza, A., et al.: 2007a, *Astron. Astrophys.*, **464**, 59.
Meilland, A., Millour, F., Stee, P., Domiciano de Souza, A., Petrov, R. G., Mourard, D., Jankov, S., et al.: 2007b, *Astron. Astrophys.*, **464**, 73.
Meilland, A., Millour, F., Stee, Ph., Spang, A., Petrov, R., Bonneau, D., Perraut, K., Massi, F.: 2008, *Astron. Astrophys.*, **488**, L67.
Meilland, A., Stee, Ph., Chesneau, O., Jones, C.: 2009, *Astron. Astrophys.*, **505**, 687.
Meilland, A., Millour, F., Kanaan, S., Stee, P., Petrov, R. et al.: 2011, *Astron. Astrophys.*, accepted.
Meisenheimer, K., Tristram, K. R. W., Jaffe, W., Israel, F., Neumayer, N., et al.: 2007, *Astron. Astrophys.*, **471**, 453.
Mennesson, B., Perrin, G., Chagnon, G., du Coudé Foresto, V., Ridgway, S., et al.: 2002, *Astrophys. J.*, **579**, 446.
Mennesson, B., Koresko, C., Creech-Eakman, M. J., Serabyn, E., Colavita, M. M., et al.: 2005, *Astrophys. J.*, **634**, L169.
Mérand, A., Kervella, P., Coudé Du Foresto, V., Ridgway, S. T., Aufdenberg, J. P., et al.: 2005, *Astron. Astrophys.*, **438**, L9.
Mérand, A., Kervella, P., Coudé Du Foresto, V., Perrin, G., Ridgway, S. T., et al.: 2006, *Astron. Astrophys.*, **453**, 155.
Mérand, A., Aufdenberg, J. P., Kervella, P., Foresto, V. Coudé du, ten Brummelaar, T. A., et al.: 2007, *Astrophys. J.*, **664**, 1093.
Millan-Gabet, R., Schloerb, F. P., Traub, W. A., Malbet, F., Berger, J. P., Bregman, J. D.: 1999, *Astrophys. J.*, **513**, L131.
Millan-Gabet, Rafael, Schloerb, F. Peter, Traub, Wesley A.: 2001, *Astrophys. J.*, **546**, 358.
Millan-Gabet, R., Pedretti, E., Monnier, J. D., Schloerb, F. P., Traub, W. A., et al.: 2005, *Astrophys. J.*, **620**, 961.
Millan-Gabet, R., Monnier, J. D., Berger, J.-P., Traub, W. A., Schloerb, F. P., et al.: 2006a, *Astrophys. J.*, **645**, L77.
Millan-Gabet, R., Monnier, J. D., Akeson, R. L., Hartmann, L., Berger, J.-P., et al.: 2006b, *Astrophys. J.*, **641**, 547.
Millan-Gabet, R., Monnier, J. D., Touhami, Y., Gies, D., Hesselbach, E., et al.: 2010, *Astrophys. J.*, **723**, 544.
Millour, F., Driebe, T., Chesneau, O., Groh, J. H.,

Hofmann, K.-H., et al.: 2009a, *Astron. Astrophys.*, **506**, L49.
Millour, F., Chesneau, O., Borges Fernandes, M., Meilland, A., Mars, G., et al.: 2009b, *Astron. Astrophys.*, **507**, 317.
Millour, F., Meilland, A., Chesneau, O., Stee, Ph., Kanaan, S., et al.: 2011, *Astron. Astrophys.*, **526**, 107.
Monnier, J. D., Millan-Gabet, R., Tuthill, P. G., Traub, W. A., Carleton, N. P., et al.: 2004, *Astrophys. J.*, **605**, 436.
Monnier, J. D., Millan-Gabet, R., Billmeier, R., Akeson, R. L., Wallace, D., et al.: 2005a, *Astrophys. J.*, **624**, 832.
Monnier, J. D., Millan-Gabet, R., Billmeier, R., Akeson, R. L., Wallace, D., et al.: 2005b, *Astrophys. J.*, **632**, 689.
Monnier, J. D., Barry, R. K., Traub, W. A., Lane, B. F., Akeson, R. L., et al.: 2006a, *Astrophys. J.*, **647**, L127.
Monnier, J. D., Berger, J.-P., Millan-Gabet, R., Traub, W. A., Schloerb, F. P., et al.: 2006b, *Astrophys. J.*, **647**, 444.
Monnier, J. D., Zhao, M., Pedretti, E., Thureau, N., Ireland, M., et al.: 2007, *Science*, **317**, 342.
Monnier, J. D., Townsend, R. H. D., Che, X., Zhao, M., Kallinger, T., et al.: 2010, *Astrophys. J.*, **725**, 1192.
Mottram, J. C., Hoare, M. G., Lumsden, S. L., Oudmaijer, R. D., Urquhart, J. S. et al.: 2007, *Astron. Astrophys.*, **476**, 1019.
Mourard, D., Bosc, I., Labeyrie, A., Koechlin, L., Saha, S.: 1989, *Nature*, **342**, 520.
Mourard, D., Bonneau, D., Koechlin, L., Labeyrie, A., Morand, F., et al.: 1997, *Astron. Astrophys.*, **317**, 789.
Mourard, D., Bério, Ph., Perraut, K., Ligi, R., Blazit, A., et al.: 2011, *Astron. Astrophys.*, **531**, 110.
Mozurkewich, D., Armstrong, J. T., Hindsley, R. B., Quirrenbach, A., Hummel, C. A., et al.: 2003, *Astron. J.*, **126**, 2502.
Muzerolle, J., Calvet, N., Hartmann, L., and D'Alessio, P.: 2003, *Astrophys. J.*, **597**, L149.
Nordgren, Tyler E., Lane, B. F., Hindsley, R. B., Kervella, P.: 2002, *Astron. J.*, **123**, 3380.
North, J. R., Davis, J., Bedding, T. R., Ireland, M. J., Jacob, A. P., et al.: 2007, *Mon. Not. R. Astron. Soc.*, **380**, L80.
O'Brien, T. J., Bode, M. F., Porcas, R. W., Muxlow, T. W. B., Eyres, S. P. S. et al. 2006, , *Nature*, **442**, 279.
Ohishi, Naoko, Nordgren, Tyler E., Hutter, Donald J.: 2004, *Astrophys. J.*, **612**, 463.
Ohnaka, K., Bergeat, J., Driebe, T., Graser, U., Hofmann, K.-H., et al.: 2005, *Astron. Astrophys.*, **429**, 1057.
Ohnaka, K., Driebe, T., Weigelt, G., Wittkowski, M.: 2007, *Astron. Astrophys.*, **466**, 1099.
Ohnaka, K., Hofmann, K.-H., Benisty, M., Chelli, A., Driebe, T., et al.: 2009, *Astron. Astrophys.*, **503**, 183.
Perrin, G., Ridgway, S. T., Coudé du Foresto, V., Mennesson, B., Traub, W. A., Lacasse, M. G.: 2004a, *Astron. Astrophys.*, **418**, 675. Betelgeuse
Perrin, G., Ridgway, S. T., Mennesson, B., Cotton, W. D., Woillez, J., et al.: 2004b, *Astron. Astrophys.*, **426**, 279. Mira
Perrin, G., Ridgway, S. T., Verhoelst, T., Schuller, P. A., Coudé Du Foresto, V., et al.: 2005, *Astron. Astrophys.*, **436**, 317.
Peterson, D. M., Hummel, C. A., Pauls, T. A., Armstrong, J. T., Benson, J. A., et al.: 2006a, *Astrophys. J.*, **636**, 1087.
Peterson, D. M., Hummel, C. A., Pauls, T. A., Armstrong, J. T., Benson, J. A., et al.: 2006b, *Nature*, **440**, 896.
Petrov, R.G.: 1988, Diffraction-Limited Imaging with Very Large Telescopes, eds. D.M. Alloin, J.M. Mariotti (Kluwer), 249.
Pijpers, F. P., Teixeira, T. C., Garcia, P. J., Cunha, M. S., Monteiro, M. J. P. F. G., Christensen-Dalsgaard, J.: 2003, *Astron. Astrophys.*, **406**, L15.
Pluzhnik, E. A., Ragland, S., LeCoroller, H., Cotton, W. D., Danchi, W. C., et al.: 2009, *Astrophys. J.*, **700**, 114.
Poncelet, A., Perrin, G., Sol, H.: 2006, *Astron. Astrophys.*, **450**, 483.
Poncelet, A., Doucet, C., Perrin, G., Sol, H., Lagage, P. O.: 2007, *Astron. Astrophys.*, **472**, 823.
Pott, J.-U., Eckart, A., Glindemann, A., Viehmann, T.: 2005, *Messenger*, **119**, 43.
Pott, J.-U., Eckart, A., Glindemann, A., Schödel, R., Viehmann, T., Robberto, M.: 2008a, *Astron. Astrophys.*, **480**, 115.
Pott, J.-U., Eckart, A., Glindemann, A., Kraus, S., Schödel, R., et al.: 2008b, *Astron. Astrophys.*, **487**, 413.
Pott, J.-U., Malkan, M. A., Elitzur, M., Ghez, A.M., Herbst,T.M. et al. 2010, *Astrophys. J.*, **715**, 736.
Preibisch, Th., Kraus, S., Driebe, Th., van Boekel, R., Weigelt, G.: 2006, *Astron. Astrophys.*, **458**, 235.
Quirrenbach, A., Hummel, C. A., Buscher, D. F., Armstrong, J. T., Mozurkewich, D., Elias, N. M., II: 1993, *Astrophys. J.*, **416**, L25.
Quirrenbach, A., Buscher, D. F., Mozurkewich, D., Hummel, C. A., Armstrong, J. T.: 1994, *Astron. Astrophys.*, **283**, L13.
Raban,D., Jaffe,W., Röttgering,H., Meisenheimer,K., Tristram,K.R.W. 2009, *Mon. Not. R. Astron. Soc.*, **394**, 1325.
Ragland, S., Traub, W. A., Berger, J.-P., Danchi, W. C., Monnier, J. D., et al.: 2006, *Astrophys. J.*, **652**, 650.
Ragland, S., Le Coroller, H., Pluzhnik, E., Cotton, W. D., Danchi, W. C., et al.: 2008, *Astrophys. J.*, **679**, 746.
Ragland, S., Akeson, R. L., Armandroff, T., Colavita, M. M., Danchi, W. C., et al.: 2009, *Astrophys. J.*, **703**, 22.
Ratzka, Th., Leinert, Ch., Henning, Th., Bouwman, J., Dullemond, C. P., Jaffe, W.: 2007, *Astron. Astrophys.*, **471**, 173.
Ravi, V., Wishnow, E. H., Townes, C. H., Lockwood, S., Mistry, H., Tatebe, K.: 2011, *Astrophys. J.*, **740**, 24.
Renard, S., Malbet, F., Benisty, M., Thiébaut, E., Berger, J.-P.: 2010, *Astron. Astrophys.*, **519**, 26.

Richichi, A., Percheron, I.: 2002, *Astron. Astrophys.*, **386**, 492.
Richichi, A., Percheron, I., Khristoforova, M.: 2005, *Astron. Astrophys.*, **431**, 773.
Roddier C. and Roddier F.: 1983, *Astrophys. J.*, **270**, L23.
Rousselet-Perraut, K., Stehlé, C., Lanz, T., Le Bouquin, J. B., Boudoyen, T., Kilbinger, M., Kochukhov, O., Jankov, S.: 2004, *Astron. Astrophys.*, **422**, 193.
Rousselet-Perraut, K., Benisty, M., Mourard, D., Rajabi, S., Bacciotti, F., et al. 2010, *Astron. Astrophys.*, **516**, L1.
Schegerer, A. A., Wolf, S., Ratzka, Th., Leinert, Ch.: 2008, *Astron. Astrophys.*, **478**, 779.
Schmitt, H. R., Pauls, T. A., Tycner, C., Armstrong, J. T., Zavala, R. T., et al.: 2009, *Astrophys. J.*, **691**, 984.
Seldin J., R. Paxman, and Keller C.: 1996, *SPIE*, **2804**, 166.
Stee, P., de Araujo, F. X., Vakili, F., Mourard, D., Arnold, L., Bonneau, D., Morand, F., Tallon-Bosc, I.: 1995, *Astron. Astrophys.*, **300**, 219.
Stee, Ph., Vakili, F., Bonneau, D., Mourard, D.: 1998, *Astron. Astrophys.*, **332**, 268.
Swain, M., Vasisht, G., Akeson, R., Monnier, J., Millan-Gabet, R., et al.: 2003, *Astrophys. J.*, **596**, L163.
Tannirkulam, A., Monnier, J. D., Millan-Gabet, R., Harries, T. J., Pedretti, E., et al.: 2008a, *Astrophys. J.*, **677**, L51.
Tannirkulam, A., Monnier, J. D., Harries, T. J., Millan-Gabet, R., Zhu, Z., et al.: 2008b, *Astrophys. J.*, **689**, 513.
Tatebe, K., Chandler, A. A., Hale, D. D. S., Townes, C. H.: 2006, *Astrophys. J.*, **652**, 666.
Tatebe, K., Wishnow, E. H., Ryan, C. S., Hale, D. D. S., Griffith, R. L., Townes, C. H.: 2008, *Astrophys. J.*, **689**, 1289.
Tatulli, E., Isella, A., Natta, A., Testi, L., Marconi, A., et al.: 2007, *Astron. Astrophys.*, **464**, 55.
Taylor, S. F., Harvin, J. A., McAlister, H. A.: 2003, *Publ. Astron. Soc. Pacific*, **115**, 609.
Thévenin, F., Kervella, P., Pichon, B., Morel, P., di Folco, E., Lebreton, Y.: 2005, *Astron. Astrophys.*, **436**, 253.
Thiebaut, E., Giovannelli, J.-F.: 2010, *IEEE Signal Processing Magazine*, **27**, 97.
Thom, C., Granes, P., Vakili, F.: 1986, *Astron. Astrophys.*, **165**, L13.
Thompson, R. R., Creech-Eakman, M. J., van Belle, G. T.: 2002a, *Astrophys. J.*, **577**, 447.
Thompson, R. R., Creech-Eakman, M. J., Akeson, R. L.: 2002b, *Astrophys. J.*, **570**, 373.
Thureau, N. D., Monnier, J. D., Traub, W. A., Millan-Gabet, R., Pedretti, E., et al.: 2009, *Mon. Not. R. Astron. Soc.*, **398**, 1309.
Tristram, K. R. W., Meisenheimer, K., Jaffe, W., Schartmann, M., Rix, H.-W., et al.: 2007, *Astron. Astrophys.*, **474**, 837.
Tristram, K. R. W., Raban, D., Meisenheimer, K., Jaffe, W., Röttgering, H., et al.: 2009, *Astron. Astrophys.*, **502**, 67.
Tuthill, P. G., Haniff, C. A., Baldwin, J. E.: 1995, *Mon. Not. R. Astron. Soc.*, **277**, 1541.
Tuthill, P. G., Haniff, C. A., Baldwin, J. E.: 1997, *Mon. Not. R. Astron. Soc.*, **285**, 529.
Tuthill P. G., Haniff C. A. and Baldwin J. E.: 1999, *Mon. Not. R. Astron. Soc.*, **306**, 353.
Tuthill, Peter G., Monnier, John D., Danchi, William C.: 2001, *Nature*, **409**, 1012.
Tuthill, P. G., Monnier, J. D., Danchi, W. C., Hale, D. D. S., Townes, C. H.: 2002, *Astrophys. J.*, **577**, 826.
Tycner, C., Hajian, A. R., Armstrong, J. T., Benson, J. A., Gilbreath, G. C., et al.: 2004, *Astron. J.*, **127**, 1194.
Tycner, C., Lester, J. B., Hajian, A. R., Armstrong, J. T., Benson, J. A., et al.: 2005, *Astrophys. J.*, **624**, 359.
Tycner, C., Gilbreath, G. C., Zavala, R. T., Armstrong, J. T., Benson, J. A., et al.: 2006, *Astron. J.*, **131**, 2710.
Vakili, F., Mourard, D., Stee, Ph., Bonneau, D., Berio, P., et al.: 1998, *Astron. Astrophys.*, **335**, 261.
van Belle, Gerard T., Ciardi, David R., Thompson, et al.: 2001, *Astrophys. J.*, **559**, 1155.
van Belle, G. T., Thompson, R. R., Creech-Eakman, M. J.: 2002, *Astron. J.*, **124**, 1706.
van Belle, G. T., Ciardi, D. R., ten Brummelaar, T., McAlister, H. A., Ridgway, S. T., et al.: 2006, *Astrophys. J.*, **637**, 494.
van Belle, Gerard T., Ciardi, David R., Boden, Andrew F.: 2007, *Astrophys. J.*, **657**, 1058.
van Boekel, R., Kervella, P., Schöller, M., Herbst, T., Brandner, W., et al.: 2003, *Astron. Astrophys.*, **410**, L37.
Vehoff, S., Hummel, C. A., Monnier, J. D., Tuthill, P., Nuernberger, D. E. A., et al.: 2010, *Astron. Astrophys.*, **520**, 78.
von Braun, K., Boyajian, T. S., Kane, S. R., van Belle, G. T., Ciardi, D. R., et al.: 2011a, *Astrophys. J.*, **729**, L26.
von Braun, K., Boyajian, T., S., ten Brummelaar, T. A., Kane, S. R., van Belle, G. T., et al.: 2011b, *Astrophys. J.*, **740**, 49.
Weigelt, G., Wittkowski, M., Balega, Y. Y., Beckert, T., Duschl, W. J. et al.: 2004, *Astron. Astrophys.*, **425**, 77.
Weigelt, G., Kraus, S., Driebe, T., Petrov, R. G., Hofmann, K.-H., et al.: 2007, *Astron. Astrophys.*, **464**, 87.
Weiner, J., Danchi, W. C., Hale, D. D. S., McMahon, J., Townes, C. H., Monnier, J. D., Tuthill, P. G.: 2000, *Astrophys. J.*, **544**, 1097.
Weiner, J., Hale, D. D. S. and Townes, C. H.: 2003, *Astrophys. J.*, **589**, 976.
Weiner, J.: 2004, *Astrophys. J.*, **611**, L37.
Weiner, J., Tatebe, K., Hale, D. D. S., Townes, C. H., Monnier, J. D., et al.: 2006, *Astrophys. J.*, **636**, 1067.
Weinberger A., Neugebauer G., and Matthews K.: 1999, *Astron. J.*, **117**, 2748.
Wilken V., de Boer C. R., Denker C., and Kneer F.: 1997, *Astron. Astrophys.*, **325**, 819.
Wilson R. W., Baldwin J. E., Buscher D. F. and Warner P. J.: 1992, *Mon. Not. R. Astron. Soc*, **257**, 369.
Wilson R. W., Dhillon V. S. and Haniff C. A.: 1997, *Mon. Not. R. Astron. Soc.*, **291**, 819.
Wittkowski M., Balega Y., Beckert T., Duschi W., Hofmann K., and Weigelt G.: 1998, *Astron. Astrophys.*, **329**, L45.

Wittkowski, M., Aufdenberg, J. P., Kervella, P.: 2004a, *Astron. Astrophys.*, **413**, 711.
Wittkowski, M., Kervella, P., Arsenault, R., Paresce, F., Beckert, T., Weigelt, G.: 2004b, *Astron. Astrophys.*, **418**, L39.
Wittkowski, M., Boboltz, D. A., Ohnaka, K., Driebe, T., Scholz, M.: 2007, *Astron. Astrophys.*, **470**, 191.
Wittkowski, M., Boboltz, D. A., Driebe, T., Le Bouquin, J.-B., Millour, F., et al.: 2008, *Astron. Astrophys.*, **479**, L21.
Woodruff, H. C., Eberhardt, M., Driebe, T., Hofmann, K.-H., Ohnaka, K., et al.: 2004, *Astron. Astrophys.*, **421**, 703.
Yoon, J., Peterson, D. M., Zagarello, R. J., Armstrong, J. Thomas, P.: 2008, *Astrophys. J.*, **681**, 570.
Young, J. S., Baldwin, J. E., Boysen, R. C., Haniff, C. A., Lawson, P. R., et al: 2000, *Mon. Not. R. Astron. Soc.*, **315**, 635.
Zhao, M., Monnier, J. D., Torres, G., Boden, A. F., Claret, A., et al.: 2007, *Astrophys. J.*, **659**, 626.
Zhao, M., Gies, D., Monnier, J. D., Thureau, N., Pedretti, E., et al.: 2008, *Astrophys. J.*, **684**, L95.
Zhao, M., Monnier, J. D., Pedretti, E., Thureau, N., Mérand, A., et al.: 2009, *Astrophys. J.*, **701**, 209.

АСТРОНОМСКА ОПТИЧКА ИНТЕРФЕРОМЕТРИЈА. II АСТРОФИЗИЧКИ РЕЗУЛТАТИ

S. Jankov

Astronomical Observatory, Volgina 7, 11060 Belgrade 38, Serbia
E–mail: *sjankov@aob.rs*

УДК 520.36–14
Прегледни рад по позиву

Оптичка интерферометрија улази у ново доба са неколико земаљских опсерваторија које, користећи дугачке интерферометријске базе, врше посматрања са просторном резолуцијом без преседана. Засноване на великом скоку унапред у квалитету и квантитету интерферометријских података, астрофизичке примене нису више ограничене само на класичне теме, као што су одређивање фундаменталних параметара звезда; наиме њихове ефективне температуре, пречници, сјај и масе, него је садашњи брзи развој на том пољу дозволио да се дође у ситуацију где оптичка интерферометрија постаје општи алат за проучавање многих астрофизичких проблема. Нарочито је улазак у употребу интерферометара са дугачким базама, који користе телескопе врло великих апертура, отворио пут за проучавање слабих објеката, тако да су први екстрагалактички резултати постали реалност. Прва декада XXI века је такође обележена синтезом апертура у видљивом и блиском инфрацрвеном домену таласних дужина, омогућавајући реконструкцију слике од површине звезда до активних галактичких језгара. Овде дајем преглед бројних до данас остварених астрофизичких резултата, изузимајући астрометрију двојних и вишеструких звезда са прецизношћу од мили-лучне секунде, која би требало да буде тема независног детаљног прегледа, узевши у обзир њену важност и очекиване резултате на нивоу микро-лучне секунде. Резултатима који су добијени тренутно доступним интерферометрима, придружујем коришћене инструменталне конфигурације да бих навео потенцијалне кориснике на одговарајуће инструменте који могу бити употребљени да би се добила жељена астрофизичка информација.